

# Spread Supersymmetry with $\tilde{W}$ LSP: Gluino and Dark Matter Signals

Lawrence J. Hall<sup>a</sup>, Yasunori Nomura<sup>a,b</sup>, and Satoshi Shirai<sup>a</sup>

<sup>a</sup> *Berkeley Center for Theoretical Physics, Department of Physics,  
and Theoretical Physics Group, Lawrence Berkeley National Laboratory,  
University of California, Berkeley, CA 94720, USA*

<sup>b</sup> *Center for Theoretical Physics, Laboratory for Nuclear Science, and Department of Physics,  
Massachusetts Institute of Technology, Cambridge, MA 02139, USA*

## Abstract

The discovery of a Higgs boson near 125 GeV, together with the absence of LHC signals for supersymmetry or direct detection signals of dark matter, motivate further study of a particular theory of split supersymmetry. In arguably the theoretically simplest implementation of split, the superpartner spectrum is spread over several decades. The squarks and sleptons are heavier than the gravitino and Higgsinos by a factor  $M_{\text{Pl}}/M_*$ , where  $M_*$  is the mediation scale of supersymmetry breaking and is high, between unified and Planck scales. On the other hand the gaugino masses are 1-loop smaller than the gravitino and Higgsino masses, arising from both anomaly mediation and a Higgsino loop. Wino dark matter arises from three sources: gravitino production by scattering at high temperatures, gravitino production from squark decays, and thermal freeze-out. For reheating temperatures larger than the squark mass, these conspire to require that the squarks are lighter than about  $10^4$  TeV, while collider limits on gaugino masses require squarks to be heavier than about 100 TeV. Whether winos constitute all or just a fraction of the dark matter, a large fraction of the allowed parameter space has the gluino within reach of the LHC with  $0.1 \text{ mm} < c\tau_{\tilde{g}} < 10 \text{ cm}$ , leading to displaced vertices. In addition, events with cascades via  $\tilde{W}^\pm$  lead to disappearing charged tracks with  $c\tau_{\tilde{W}^\pm} \sim 10 \text{ cm}$ . The squarks and sleptons are predicted to be just heavy enough to solve the supersymmetric flavor and  $CP$  problems. Thus gluino decay modes may typically violate flavor and involve heavy quarks:  $[\bar{t}(t, c, u) + \bar{b}(b, s, d)]\tilde{W}^0$  and  $[\bar{t}(b, s, d) + (\bar{t}, \bar{c}, \bar{u})b]\tilde{W}^\pm$ . The electron electric dipole moment is expected to be of order  $10^{-29} e \text{ cm}$ , two orders of magnitude below the current limit. The AMS-02 search for cosmic ray antiprotons will probe an interesting region of parameter space.

# 1 Introduction

All realistic theories of supersymmetry have supersymmetry breaking in a hidden sector—the key question is how this breaking is mediated to the superpartners of the standard model (SM) particles. In 4 dimensions, physics at the gravitational scale provides an almost irremovable contribution to the mediation [1], and generically leads to all SM superpartners acquiring masses of order the gravitino mass,  $m_{3/2} = F_X/\sqrt{3}M_{\text{Pl}}$ , where  $F_X$  is the leading spurion of supersymmetry breaking and  $M_{\text{Pl}}$  is the reduced Planck scale. Augmented with an approximate flavor symmetry, gravity mediation could describe supersymmetry breaking with few parameters, leading to theories where dark matter arises from freeze-out of the lightest supersymmetric particle (LSP).

Over the last 30 years, this minimal standard picture of gravity mediation met a succession of challenges:

**The Supersymmetric Flavor/ $CP$  Problem** arises because it is not clear that approximate flavor symmetries will be respected by physics at the gravitational scale. However, solutions such as gauge mediation require further fields and model building, and do not allow weakly interacting massive particle (WIMP) LSP dark matter in their minimal implementations.

**A Derived Planck scale:** With extra spatial dimensions, the Planck scale is a derived scale, larger than the fundamental scale  $M_*$  by a volume factor [2]. In this case higher dimensional operators arise in the low energy effective theory from integrating out string states, leading to supersymmetry breaking masses of order  $\tilde{m} = F_X/M_*$ , dominating the purely gravitational ones. This typically yields a gravitino LSP, again precluding WIMP LSP dark matter. Furthermore, decays of the next-to-LSP to the gravitino in the early universe occur after nucleosynthesis and are generically problematic [3, 4].

**Anomaly Mediation:** A hidden assumption of gravity mediation is that the field  $X$  of the supersymmetry breaking sector is neutral under all symmetries. If it is charged under some symmetry, operators linear in  $X$  leading to gaugino masses and the  $\mu$  parameter are absent, so that the leading supersymmetry breaking in the SM sector is for scalar mass terms only. The dominant contribution to gaugino masses arises at 1-loop via the superconformal anomaly [5, 6], yielding an  $O(\alpha/4\pi)$  hierarchy between scalar and fermion superpartner masses that destroys the supersymmetric solution to the hierarchy problem. One can either attempt to regain naturalness by suppressing the contribution from gravity mediation by sequestering [5], or one can accept that the theory possesses a few orders of magnitude of fine-tuning [6, 7].

**Split Supersymmetry:** The environmental requirement of structure formation allows a multiverse solution to the cosmological constant problem [8, 9]; similarly, the requirement of stable complex nuclei allows a multiverse solution to the hierarchy problem [10]. Furthermore, both environmental arguments become plausible in the context of the string landscape [11]. While a multiverse solution to the hierarchy problem decouples the scale of supersymmetry breaking from the weak scale, the fermionic superpartners have chiral symmetries that could allow them to be

much lighter than the scalar superpartners to account for dark matter, yielding a highly split spectrum of superpartners [12]. A variety of split spectra yield gauge coupling unification that is as precise as natural supersymmetric theories.

How does the discovery of a Higgs boson near 125 GeV, and the absence of signals for supersymmetry so far, affect our view of the mediation of supersymmetry breaking? Certainly there is no unique answer—at one extreme high scale supersymmetry [13], with the SM valid to unified scales, remains a possibility if  $\tan\beta$  is close to unity, and at the other extreme there are several possibilities for natural electroweak symmetry breaking that allow superpartners to evade current LHC searches [14]. However, there is a very simple scenario that addresses all four of the above challenges, is well-motivated by LHC results to date, and has highly distinctive LHC and astrophysical signals.

The first key assumption is that the field  $X$  carries some symmetry so that, from the above discussion, the superpartner spectrum has a modest degree of splitting from two sources:

- Gaugino masses arising from anomaly mediation are  $O(\alpha/4\pi)$  suppressed relative to scalar superpartner masses.
- Gaugino and Higgsino masses arising only from gravitational effects are  $O(M_*/M_{\text{Pl}})$  suppressed relative to scalar superpartner masses.

If these are the only sources of splitting, the spectrum of the “Simplest Model of Split Supersymmetry” [15] results—the case we study in this paper.

With this moderately split spectrum, the weak scale is fine-tuned by several orders of magnitude, making plausible the second key assumption:

- The overall normalization of the superpartner spectrum is determined by an environmental requirement on the abundance of dark matter.

This selection in the multiverse (or quantum many universes [16]) has an important implication—dark matter might be multi-component, for example with roughly comparable contributions from LSPs and axions. This will have the effect of increasing the range of parameters that yields signals at the LHC. Taken together, the above three items define what we mean by “Spread Supersymmetry” [17].

If  $X$  is neutral under all symmetries, differentiating  $M_*$  from  $M_{\text{Pl}}$  leads to the expectation of a gravitino LSP. However, taking  $X$  charged leads instead to either a gaugino or Higgsino LSP. The origin of the Higgsino mass is critical since it determines whether the LSP is gaugino or Higgsino, leading to two realistic versions of Spread Supersymmetry with neutral wino or Higgsino dark matter. In this paper we assume the Higgsino mass is of order  $m_{3/2}$  so that the LSP is wino, since only in this case are we led to interesting gluino signals at the LHC. This can arise from supergravity interactions that follow from having  $H_u H_d$  in the Kähler potential [18] or that cause a readjustment of the vacuum [19, 20].

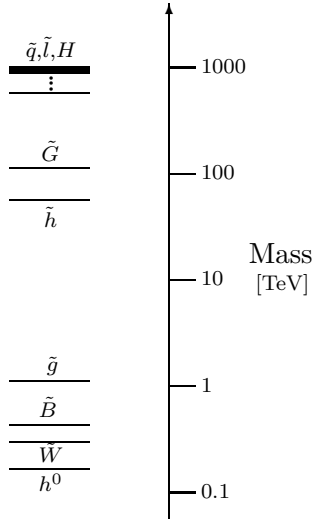


Figure 1: Typical spectrum of Spread Supersymmetry with wino LSP.

Hence, we study a supersymmetric theory with minimal field content and leading supersymmetry breaking effects arising from

$$\mathcal{L}_{\text{SB}} \sim \frac{1}{M_*^2} [X^\dagger X (\Phi^\dagger \Phi + H_u H_d)]_{\theta^4} + [H_u H_d]_{\theta^4} - \frac{m_{3/2}}{2} \left( \tilde{G} \tilde{G} + \frac{b_a \alpha_a}{4\pi} \lambda_a \lambda_a \right), \quad (1)$$

where  $\Phi$  are the chiral superfields,  $H_u, H_d$  are the Higgs superfields,  $\tilde{G}$  is the gravitino,  $\lambda_a$  are the gauginos, and  $b_a$  and  $\alpha_a$  are the 1-loop beta function coefficients and gauge coupling strengths for  $a = U(1)_Y, SU(2)_L, SU(3)_C$ . Here, we have omitted the chiral compensator field  $\phi = 1 + m_{3/2} \theta^2$ , which is important in the second term leading to the supersymmetric Higgs mass  $\mu$  of order  $m_{3/2}$ , and each operator (except for the  $\tilde{G}$  and  $\lambda_a$  mass terms) should be understood to have an unknown coefficient of order unity that is not displayed. The resulting superpartner masses have a moderate hierarchy

$$(\tilde{q}, \tilde{l}, H) : (\tilde{G}, \tilde{h}) : \lambda_a \approx \tilde{m} : m_{3/2} : \frac{\alpha_a}{4\pi} m_{3/2}, \quad (2)$$

as depicted in Fig. 1. Here  $H$  is the heavy Higgs doublet orthogonal to the doublet that has been fine-tuned to be at the weak scale.

Many aspects of a moderately split supersymmetric spectrum have been noted and studied before. In particular, anomaly mediation triggered the first papers to take seriously the unpopular idea of a few orders of magnitude of fine-tuning [6, 7], and also triggered studies of wino dark matter [21, 22, 23, 24]. The possibility of combining this with a modest hierarchy from  $M_*/M_{\text{Pl}}$  to yield a solution to the flavor problem was mentioned in [12], together with the possibility of long-lived gluinos. Implications of this scenario on thermal WIMP dark matter, especially the possibility of having dark matter with significant mass degeneracy between a bino and wino, were studied in [15]. It is well-known that once the gravitino mass is above 10 TeV there is no cosmological

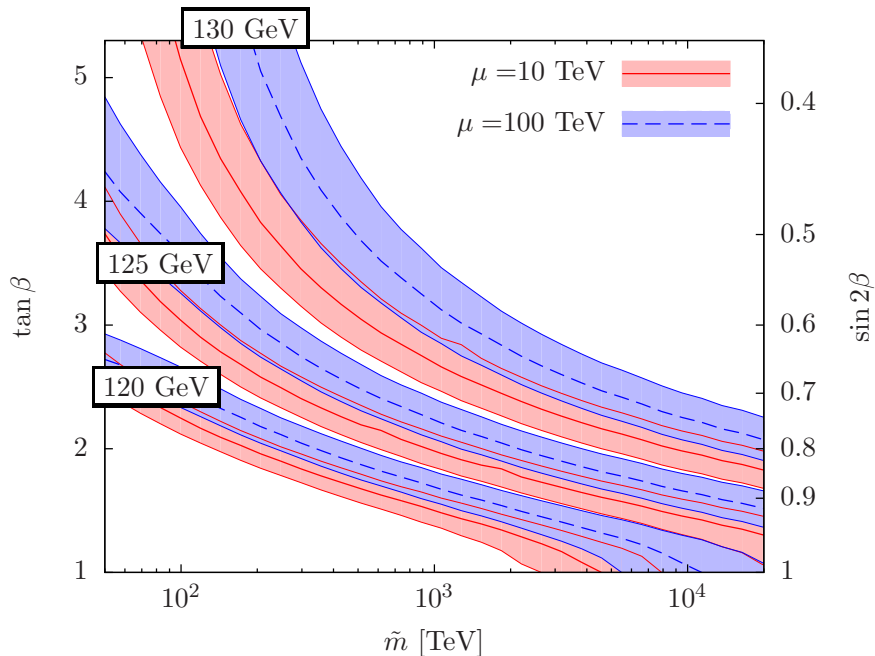


Figure 2: The values of the Higgs boson mass in the  $\tilde{m}$ - $\tan\beta$  plane. The solid (red) curves represent ones with  $\mu = 10$  TeV, while the dashed (blue) curves  $\mu = 100$  TeV. The shaded region around each curve shows uncertainty from the top quark mass. For the gaugino masses, we have set  $M_1 = 600$  GeV,  $M_2 = 300$  GeV, and  $M_3 = 2000$  GeV.

gravitino problem, and similarly a moderately split spectrum solves possible moduli and proton decay problems. LHC signatures of wino LSP were studied in [25, 26], and aspects of particle physics and cosmology of a moderately split spectrum with  $M_* = M_{\text{Pl}}$  were discussed recently in a series of papers in [27].

Dark matter is a critical aspect of Spread Supersymmetry since it determines the normalization of the entire superpartner spectrum. It constrains the scale of the squark masses to be in the range

$$\tilde{m} \sim (10^2 - 10^4) \text{ TeV}. \quad (3)$$

The upper limit follows from freeze-in of dark matter via gravitinos [28, 29], assuming  $T_R > \tilde{m}$ , and the lower limit from requiring gravitinos to decay before the Big-Bang nucleosynthesis (BBN). Furthermore, from Eq. (1) all entries in the Higgs mass-squared matrix are comparable, so that  $\tan\beta$  is not expected to be large. Since the top squark mixing parameter vanishes at tree level, the Higgs boson mass is determined essentially only by  $(\tilde{m}, \tan\beta)$ , which is shown in Fig. 2. The measurement of the Higgs mass at the LHC is a key motivation for studying the predictions of this theory in some detail.

In theories with wino LSP arising from anomaly mediation, it is generally understood that the wino mass should be near 3 TeV, so that thermal freeze-out can account for the observed dark matter, leading to a gluino heavier than 5 TeV that is out of the LHC reach. In this paper we

show that in Spread Supersymmetry the situation is different: there is a large fraction of parameter space where the gluino is light enough to be discovered at the LHC. There are two reasons for this reduction in the wino and gluino masses. Firstly dark matter production also occurs via gravitino production, from both freeze-in from squark decay and UV gluino scattering. Secondly, the winos might account for only a fraction of the observed dark matter, as discussed below. Both these effects require a lower wino mass. Another consequence of the lighter wino is the change in the indirect cosmic ray signals for dark matter. The photon signal already excludes winos lighter than about 500 GeV constituting all the dark matter, and antiproton signals will soon provide an additional probe of the theory.

The lifetime of the gluino reaches  $c\tau_{\tilde{g}} \approx 10$  m, for  $\tilde{m}$  at the upper limit of Eq. (3) for a 1 TeV gluino mass, suggesting an exciting possibility of displaced vertices from gluino decays [12]. However, the lifetime scales as  $\tilde{m}^4$  and hence a detailed analysis of dark matter production, including freeze-out, freeze-in, and UV scattering, is required to predict the allowed range of  $c\tau_{\tilde{g}}$ . Such an analysis will also yield the precise allowed range of  $\tilde{m}$ , estimated at the order of magnitude level in Eq. (3), giving an indication of the likelihood of flavor and  $CP$  violating signals in this theory.

In the context of the multiverse, the abundance of dark matter can serve an important environmental factor that affects the selection of parameters of the theory in our universe. In particular, this may choose the initial misalignment angle of the axion field—which we expect to exist because of the strong  $CP$  problem—yielding axion dark matter [30]. In Spread Supersymmetry, the same mechanism can act on the combined abundance of relic WIMPs and axions, leading generically to multi-component dark matter. The precise ratio of the two components depends on the a priori distribution of parameters in the landscape [17]. We, however, expect in general that the LSP abundance is *bounded* by the observed dark matter abundance,  $\Omega_{\tilde{W}} < \Omega_{\text{DM}}$ , not necessarily saturates it, although how much  $\Omega_{\tilde{W}}$  deviates from  $\Omega_{\text{DM}}$  depends on the a priori probability distribution of parameters.

The organization of this paper is as follows. In Section 2, we study particle physics aspects of the model. We describe the detailed spectrum of superpartners and the Higgs boson, and analyze collider signals as well as physics of flavor and  $CP$  violation. We find that the model naturally leads to a distinct signal of a long-lived gluino decaying into a long-lived charged wino, decaying into the neutral wino LSP. The model also allows for interesting handles of the flavor structure in the scalar sector at  $\tilde{m} \sim (10^2 - 10^4)$  TeV through observations of gluino decays. In Section 3, we study astrophysical and cosmological aspects of the model. We find that, because of relatively large  $\tilde{m}$ , the freeze-in contribution to  $\Omega_{\tilde{W}}$  is generally important. We also consider the UV scattering and thermal contributions, and discuss their effects on the cosmology of the model. In Section 4, we combine these results and study current constraints on the model as well as future prospects for a discovery. We find that while some of the parameter space is already constrained by the current LHC and Fermi data, there are large parameter regions still unconstrained, some of which is compatible with thermal leptogenesis at high temperatures. We find that future data from the

LHC, searches of electric dipole moments, and astrophysical observations have good potentials to discover signals of the model. In Section 5, we discuss how the current model may arise from environmental selection in the multiverse. Finally, we conclude in Section 6.

## 2 Particle Physics

In this section we discuss particle physics aspects of Spread Supersymmetry with wino LSP. We first describe the detailed spectrum of the theory, and then discuss physics at colliders and of flavor and  $CP$  violations.

### 2.1 Mass spectrum

We assume that the supersymmetry breaking field  $X$  is charged under some symmetry. While this suppresses the operators linear in  $X$ , it still allows  $X^\dagger X$  to couple to any SM singlet operators; in particular, it allows the Kähler potential terms

$$K \ni -\frac{c}{M_*^2} X^\dagger X \Phi_{\text{MSSM}}^\dagger \Phi_{\text{MSSM}}, \quad (4)$$

where  $\Phi_{\text{MSSM}} = \Phi_M, H_u, H_d$ , and  $c = O(1)$  represents generic coefficients, which may depend on the species. This leads to the soft masses  $\tilde{m}^2 = c|F_X|^2/M_*^2$  for the minimal supersymmetric standard model (MSSM) scalars. Here,  $M_*$  is the cutoff scale of the theory, which we take to be larger than the supersymmetric unification scale,  $\approx 10^{16}$  GeV, to preserve supersymmetric gauge coupling unification in its simplest form.<sup>1</sup>

We expect scale  $M_*$  to be smaller than the 4D reduced Planck scale,  $M_{\text{Pl}}$ . For example, if there is a small extra  $d$ -dimensional space around these scales, then we have  $M_{\text{Pl}}^2 \approx M_*^{2+d} V > M_*^2$ , where  $V$  is the volume of the extra compact space; more generally, if there are  $N \gg 1$  species that are effectively massless around these scales, then we expect  $M_{\text{Pl}}^2 \approx N M_*^2 > M_*^2$  [31]. This implies that the scalar masses  $\tilde{m} \approx F_X/M_*$  is expected to be somewhat larger than the gravitino mass  $m_{3/2} = F_X/\sqrt{3}M_{\text{Pl}}$ . For later convenience, we define

$$r_* \equiv \frac{\sqrt{3}M_{\text{Pl}}}{M_*} \approx \frac{\tilde{m}}{m_{3/2}}. \quad (5)$$

In this paper we mainly consider the range  $1 \lesssim r_* \lesssim O(100)$ .

Let us now discuss the Higgs sector. If  $H_u H_d$  is neutral, which we assume here, then we can have operators

$$K \ni -\frac{c'}{M_*^2} X^\dagger X H_u H_d + c'' H_u H_d + \text{h.c.}, \quad (6)$$

---

<sup>1</sup>If  $M_*$  is too close to the unification scale, we may expect significant threshold corrections from higher dimension operators.

which generate the holomorphic supersymmetry-breaking Higgs mass-squared  $b = c'|F_X|^2/M_*^2$  as well as the supersymmetric Higgs mass  $\mu = c''m_{3/2}^*$ . Unlike the soft scalar masses, the supersymmetric  $\mu$  term is of order the gravitino mass.<sup>2</sup> The size of the  $b$  term is of the same order as the soft scalar mass-squared, which implies that  $\tan\beta \equiv \langle H_u \rangle / \langle H_d \rangle = O(1)$ .

Direct couplings of  $X$  to the gauge supermultiplets are forbidden by the symmetry, so that the main contribution to the gaugino masses arise from anomaly mediation. In addition, the electroweak gauginos obtain masses of comparable size from loops of the Higgsino and Higgs bosons. The gaugino mass parameters are then given by

$$M_1 = \frac{3}{5} \frac{\alpha_1}{4\pi} (11m_{3/2} + L), \quad (7)$$

$$M_2 = \frac{\alpha_2}{4\pi} (m_{3/2} + L), \quad (8)$$

$$M_3 = \frac{\alpha_3}{4\pi} (-3m_{3/2})(1 + c_{\tilde{g}}). \quad (9)$$

Here,  $L$  represents the correction from Higgsino-Higgs loops:

$$L = \mu \sin(2\beta) \frac{m_A^2}{|\mu|^2 - m_A^2} \ln \frac{|\mu|^2}{m_A^2} \sim 2\mu \sin(2\beta) \ln r_*, \quad (10)$$

with  $m_A = O(\tilde{m})$  being the heavy Higgs boson mass.  $c_{\tilde{g}}$  is the logarithmic correction from the heavy squarks, which at the one-loop level is given by

$$1 + c_{\tilde{g}} = \left( 1 + \frac{5\alpha_3(|M_3|)}{4\pi} \ln \frac{m_{\tilde{q}}}{|M_3|} \right)^{4/5}, \quad (11)$$

with  $m_{\tilde{q}} = O(\tilde{m})$  being the squark mass which we have taken to be universal here. In the expressions above and throughout the paper, we adopt the phase convention that the gravitino mass  $m_{3/2}$  and  $\tan\beta$  are real and positive, while  $\mu$  has a complex phase in general. Note that we can always take this convention by appropriate phase rotations of the fields.

The gauginos are lightest among all the superparticles. The condition  $m_{\text{gaugino}} \gtrsim 100$  GeV then indicates  $m_{3/2} > O(10 \text{ TeV})$ , so that the scalar masses are  $\tilde{m} \approx r_* m_{3/2}$ , which are typically of order  $10^2 - 10^4$  TeV. Such heavy scalars predict a relatively large SM-like Higgs boson mass  $m_h$ . In fact, we find that the suggested values of  $\tan\beta = O(1)$  and  $\tilde{m} = O(10^2 - 10^4 \text{ TeV})$  naturally realize the 125 GeV Higgs boson as seen in Fig. 2. (Note that scalar trilinear interactions are generated only by anomaly mediation and thus are small  $A = O(m_{3/2}/16\pi^2) \ll \tilde{m}$ .)

Phenomenology of the model depends strongly on which gaugino is the LSP. As seen in Eqs. (7–9), the relative values of the gaugino masses depend on the size of  $L$ . Since  $L$  can be relatively large in the present model because of large  $r_*$ , in principle any gaugino can be the LSP. However, if  $R$ -parity conservation is assumed, the LSP is stable and contributes to the dark matter. In this

---

<sup>2</sup>We assume there is no superpotential term of the form  $W = H_u H_d \langle W \rangle / M_*^2$ , where  $\langle W \rangle$  is the expectation value of the superpotential needed to cancel the cosmological constant, which would lead to  $\mu = O(m_{3/2} M_{\text{Pl}}^2 / M_*^2)$ .



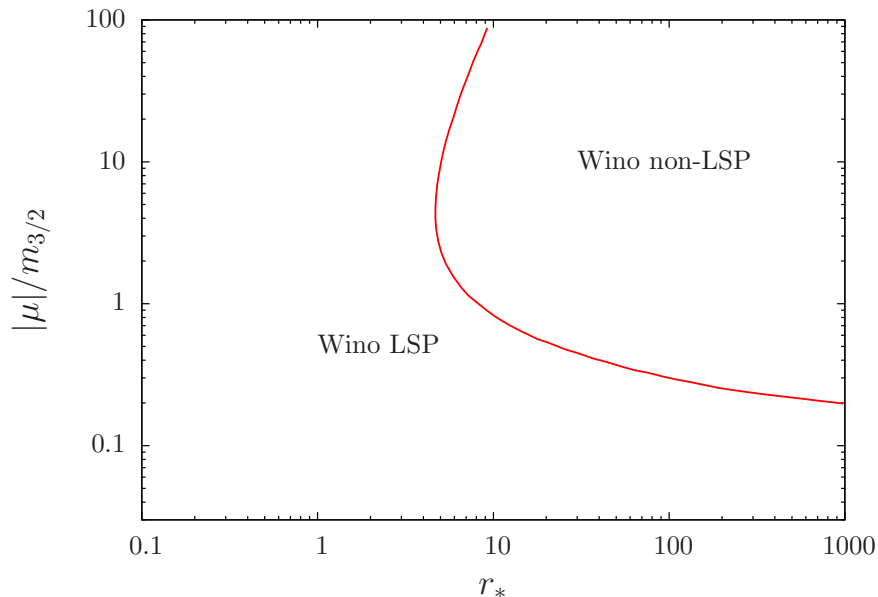


Figure 3: The wino LSP region in the  $r_*$ - $|\mu|/m_{3/2}$  plane. In the “Wino LSP” region, an appropriate choice of  $\arg(\mu)$  allows the wino LSP, while in the “Wino non-LSP” region, no choice of  $\arg(\mu)$  leads to the wino LSP.

case the gluino LSP is excluded. In the case of the bino LSP, its thermal relic abundance is roughly given by

$$\Omega_{\tilde{B}} h^2 \sim O(10^{2-3}) \times \left( \frac{|\mu|}{10 \text{ TeV}} \right)^2 \quad (12)$$

for  $\tan \beta \sim 1$  and  $|M_1| \ll |M_2|$ , where  $h \simeq 0.7$  is the present-day Hubble expansion rate in units of  $\text{km s}^{-1} \text{Mpc}^{-1}$ . The precise value depends on details, especially the phase of  $M_1 \mu$  since its imaginary part contributes to  $s$ -wave annihilation, but the value suggested by Eq. (12) is much larger than the observed dark matter abundance for a natural parameter region,  $|\mu| = O(m_{3/2})$ . Therefore, we focus on the case of the wino LSP in this paper.<sup>3</sup>

The requirement of the wino LSP constrains the size of  $|\mu|$ , depending on the value of  $r_*$ , as can be seen from Eq. (10). In Fig. 3, we show the region in which the LSP is the wino in the  $r_*$ - $|\mu|/m_{3/2}$  plane. Here, we have set  $m_{3/2} = 100 \text{ TeV}$  and the phase of  $\mu$  is chosen such that  $|M_2| - |M_1|$  is minimized. The value of  $\tan \beta$  is chosen to realize the 125 GeV Higgs boson. (In the region where no solution for  $\tan \beta$  exists, we have set  $\tan \beta = 1$ .)

<sup>3</sup>If the bino mass is about 60 GeV and its annihilation hits the 125 GeV Higgs boson pole, then the size of  $\mu$  can be as large as a few TeV without a  $CP$  violating phase, avoiding overabundance. If  $|M_2| - |M_1|$  is small, coannihilation process is effective [15], and the bino LSP is allowed. In this case,  $(|M_2| - |M_1|)/|M_1| < O(10\%)$  is required.

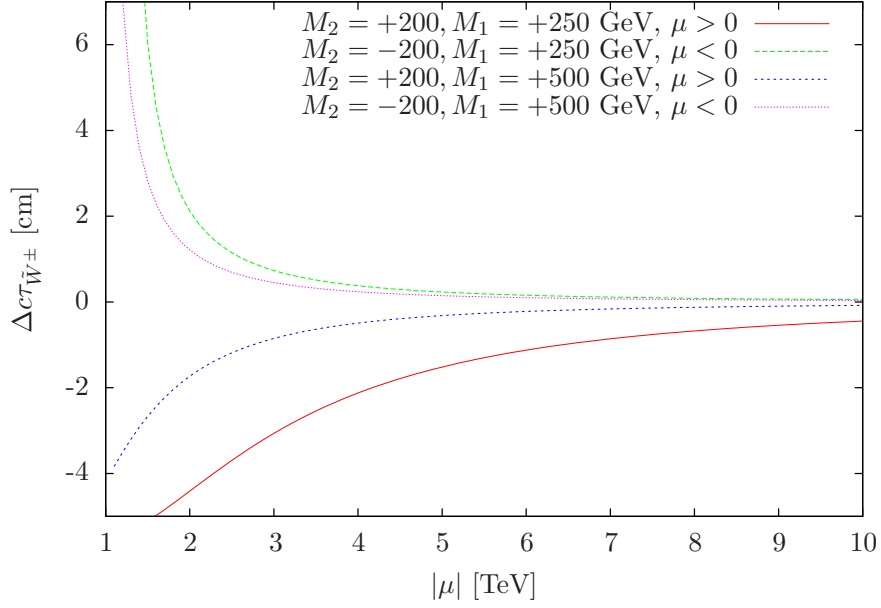


Figure 4:  $\Delta c\tau_{\tilde{W}^\pm} = c\tau_{\tilde{W}^\pm} - c\tau_{\tilde{W}^\pm}^{|\mu| \rightarrow \infty}$  as a function of  $|\mu|$  for various values of  $M_1$  and  $M_2$ . We have set  $\sin(2\beta) = 1$ .

## 2.2 Collider signals

As in any models in which the gaugino masses arise mainly from anomaly mediation and in which  $\mu$  is sufficiently larger than the gaugino masses, the present model has the neutral wino LSP and the charged wino next-to-LSP nearly degenerate. For  $|\mu| = O(m_{3/2})$ , the small mass difference between the charged and neutral winos is determined by the electromagnetic loop contribution:  $\delta M = M_{\tilde{W}^\pm} - M_{\tilde{W}^0} \simeq 160$  MeV. This small mass splitting makes the decay length of the charged wino relatively long,  $c\tau \approx O(10$  cm), and make it potentially observable at the LHC [25]. Note, however, that in the present model, larger  $r_*$  generically implies relatively small  $|\mu|$  (though still of order  $m_{3/2}$ ) and  $\tan\beta$ , because of the constraint from the wino LSP and the Higgs mass. In this case, the tree-level contribution to the mass splitting can be important, which can be written as

$$(\delta M)^{\text{tree}} \simeq \frac{m_W^4 t_W^2 \sin^2(2\beta)}{|\mu|^2 (|M_1|^2 - |M_2|^2)} \{ |M_2| + |M_1| \cos(\arg(M_1 M_2 \mu^2)) \}, \quad (13)$$

where  $t_W$  is the tangent of the Weinberg angle. In fact, for small  $|\mu|$  and/or  $|M_1| \sim |M_2|$ , the effect of this contribution on the decay width of the charged wino is sizable. In Fig. 4, we show the deviation of  $c\tau_{\tilde{W}^\pm}$  from  $c\tau_{\tilde{W}^\pm}^{|\mu| \rightarrow \infty}$ .

As we will see later, a significant portion of the Spread Supersymmetry parameter region allows for production of gluinos at the LHC. Once produced, the gluino decays through the exchange of heavy squarks. Therefore, the modes and rate of gluino decay can provide important information on the squark sector. In the present model, the dominant decay modes are three-body decay  $\tilde{g} \rightarrow q\bar{q}\chi$ , and the two-body decay process  $\tilde{g} \rightarrow g\chi$  is strongly suppressed [32, 33]. This therefore

Table 1: Current lower bounds on the gluino mass.

$c\tau_{\tilde{g}}$	Bound on $M_{\tilde{g}}$ [GeV]	References
Prompt	700 – 1200	[35] (multi-jets + missing), [36] ( $b$ jets + missing), ...
30 m	500	[37] (stopped gluino)
300 m	600	[37] (stopped gluino)
3000 m – $10^{12}$ m	640	[37] (stopped gluino)
$\gg 10$ m	1000 – 1100	[38] ( $R$ -hadron)

provides a good test of the model [34].

Because of  $r_* \gtrsim O(1)$ , the present model can have much heavier scalar particles than the conventional anomaly mediation model. Such heavy scalars result in a long-lived gluino, whose decay length is approximately given by

$$c\tau_{\tilde{g}} = O(1 \text{ cm}) \left( \frac{M_{\tilde{g}}}{1 \text{ TeV}} \right)^{-5} \left( \frac{\tilde{m}}{1000 \text{ TeV}} \right)^4. \quad (14)$$

This implies that  $r_*$  larger than  $\approx O(10)$  may lead to distinct long-lived gluino signatures. Together with the  $\tilde{W}^\pm$  track arising from the gluino decay, such a long-lived gluino may allow us to extract various information, such as the lifetimes of  $\tilde{W}^\pm$  and the gluino as well as the masses of the wino, bino and gluino. An interesting possibility is that the long-lived gluino may “carry” the  $\tilde{W}^\pm$  track from the collision point to the transition radiation tracker, facilitating the measurement of the  $\tilde{W}^\pm$  track.

In Table 1, we compile the current constraints on the gluino mass for various gluino decay lengths. While the accurate constraints depend on the details of the mass spectrum and decay patterns of the MSSM particles, and stopped gluino and  $R$ -hadron search are subject to different theoretical uncertainties, the lower bound on  $M_{\tilde{g}}$  is roughly in the range of  $\approx 1$  TeV.

Summarizing, Spread Supersymmetry with wino LSP has nearly degenerate neutral wino LSP and charged wino next-to-LSP, as in other models based on anomaly mediation, and the latter may be detectable as a charged track at the LHC. In addition, unlike the conventional anomaly mediation model, Spread Supersymmetry naturally leads to a long-lived gluino because of rather heavy squarks of mass  $m_{\tilde{q}} \approx r_* m_{3/2}$ . Therefore, in some decay chains, we have two long-lived particles:

$$\tilde{g} \xrightarrow{\text{long-lived}} q\bar{q}(\tilde{W}^\pm \xrightarrow{O(10 \text{ cm})} \tilde{W}^0 \pi^\pm), \quad (15)$$

allowing for an extraction of information about the masses and lifetimes of these particles. Note that this signature, although exotic, is a natural consequence of the model, and occurs quite generically. The measurement of this type of gluino decay may also reveal information on the squark sector, especially the scale of the squark masses.

## 2.3 Flavor and $CP$

The heavier scalar mass spectrum is favorable from the viewpoint of the supersymmetric flavor and  $CP$  problems. The ultraviolet physics at  $M_*$  need not respect the SM flavor symmetry, in which case large flavor violating soft masses are expected. To suppress low energy flavor violating processes, large  $\tilde{m}$  is then required. For example, suppressing  $\Delta F = 2$  mixing between the first and second generation quarks requires  $\tilde{m} > O(10^3 \text{ TeV})$ , and that for the first and third requires  $\tilde{m} > O(10^2 \text{ TeV})$  [39]. With  $r_* > 1$ , the present model can have sufficiently heavy scalar masses to avoid constraints from low-energy flavor violating processes, even if they have maximal flavor violation. On the other hand, because we expect  $r_* < O(100)$ , some deviations from the SM may be observed in future flavor experiments.

The gluino decay is sensitive to the squark masses, and its observation may provide information about the flavor violating structure of the squark masses. The gluino decays into two quarks and a lighter superparticle via a squark exchange. If the squark masses have flavor-violating structure, the gluino will decay dominantly by the exchange of the lightest squark, leading to the quarks of the corresponding flavor. Furthermore, flavor-violating decays, such as  $\tilde{g} \rightarrow b\bar{s}\tilde{\chi}, t\bar{c}\tilde{\chi}$ , are also expected to occur. By using heavy flavor tagging techniques, such a “flavorful” gluino may be identified. Detailed studies of the flavor of the quarks from gluino decays, therefore, can provide important information on the size of flavor violation in the squark sector.

We finally discuss possible signals from electric dipole moments (EDMs). New physics beyond the standard model with  $CP$  violation naturally provides large EDMs of an electron, a neutron, and so on. In the present model, one-loop contributions to the EDMs from heavy scalars are suppressed unless  $r_*$  is small, of  $O(1)$ . However, the model predicts relatively small  $\mu$ , and its phase is generically expected to be of  $O(1)$ . In this case, two-loop diagrams without scalars can give significant contributions [28]; for example, the electron EDM is given by

$$d_e \simeq 3 \times 10^{-29} e \text{ cm} \times \sin(2\beta) \sin(\arg(M_2\mu)) \left( \frac{|\mu|}{10 \text{ TeV}} \right)^{-1} \left( \frac{M_{\tilde{W}}}{200 \text{ GeV}} \right)^{-1} f(m_h^2/M_{\tilde{W}}^2), \quad (16)$$

where  $f(x) = 1 - \ln(x)/2 + (5/3 - \ln(x))x/12 + \dots$ .

The current constraint on the electron EDM is  $d_e < 1.05 \times 10^{-27} e \text{ cm}$  at 90%C.L. [40], which still does not explore an interesting region of the model. However, planned EDM experiments are expected to have a few orders of magnitude improved sensitivity [40, 41], reaching the level of  $d_e \sim 10^{-31} e \text{ cm}$ , or even smaller. These experiments will then be a good probe of the model.

## 3 Astrophysics and Cosmology

In this section, we discuss astrophysical and cosmological aspects of Spread Supersymmetry with wino LSP. We find that sizable  $r_*$  plays an important role.

### 3.1 Wino relic abundance

In the present model, the gravitino mass is larger than  $O(10 \text{ TeV})$ . Such a heavy gravitino decays before BBN, so the model does not suffer from the BBN constraints [4]. On the other hand, decays of gravitinos produced in the early universe lead to additional wino abundance after wino freeze-out. Therefore, too large primordial gravitino abundance may result in overabundance of the wino LSP.

There are two sources for the relic abundance of the wino LSP: the thermal relic contribution and the non-thermal contribution from the gravitino decay. The total wino relic abundance can thus be given by the sum of these two<sup>4</sup>

$$\Omega_{\tilde{W}} = \Omega_{\tilde{W}}^{\text{thermal}} + \Omega_{\tilde{W}}^{\text{non-thermal}}. \quad (17)$$

The thermal relic abundance is given by

$$\Omega_{\tilde{W}}^{\text{thermal}} h^2 \simeq 2 \times 10^{-4} \left( \frac{M_{\tilde{W}}}{100 \text{ GeV}} \right)^2 \quad (18)$$

without including the Sommerfeld effect, which reduces  $\Omega_{\tilde{W}}^{\text{thermal}}$  from this expression for a heavy wino,  $M_{\tilde{W}} \gtrsim \text{TeV}$  [22]. The non-thermal wino abundance is related to the primordial gravitino abundance before the decay,  $\Omega_{3/2}$ , by

$$\Omega_{\tilde{W}}^{\text{non-thermal}} = \frac{M_{\tilde{W}}}{m_{3/2}} \Omega_{3/2}, \quad (19)$$

so we need to know  $\Omega_{3/2}$  to obtain the final wino abundance,  $\Omega_{\tilde{W}}$ .

There are two main origins for the primordial gravitino abundance,  $\Omega_{3/2}$ . One comes from thermal scatterings of the MSSM particles at the reheating era, which becomes important if the reheating temperature  $T_R$  is high, e.g.,  $\gtrsim 10^8 \text{ GeV}$ .<sup>5</sup> In this case (more specifically if  $T_R \gtrsim O(10 \tilde{m})$ ), the contribution depends almost only on  $T_R$  and is well fitted by [42]

$$\Omega_{3/2}^{\text{UV}} h^2 \simeq 3.9 \left( \frac{T_R}{10^9 \text{ GeV}} \right) \left( \frac{m_{3/2}}{100 \text{ TeV}} \right). \quad (20)$$

(This contribution, however, suffers from some theoretical uncertainties; for example, the procedure of Ref. [43] gives about two times larger abundance than the one in Eq. (20).) Another one comes

---

<sup>4</sup>If the gravitino mass is large and the wino mass small, then late-time annihilation after the gravitino decay can be effective, making the final wino abundance smaller. If the gravitino mass is 500 TeV (2000 TeV) and the wino mass 100 GeV (500 GeV), for example, this leads to a deviation from the simple sum in Eq. (17) by about 10%. In the rest of the paper, we ignore this effect for simplicity since it is not significant in relevant parameter space.

<sup>5</sup>We define the reheating temperature by

$$T_R \equiv \left[ \frac{90}{\pi^2 g_*(T_R)} \Gamma_{\text{inf}}^2 M_{\text{Pl}}^2 \right]^{1/4},$$

where  $\Gamma_{\text{inf}}$  is the decay rate of the inflaton field and  $g_*$  is the number of effective massless degrees of freedom.

from the freeze-in contribution. This contribution arises if  $T_R$  is larger than the scalar masses  $\tilde{m}$ , and depends almost only on  $\tilde{m}$ :

$$\Omega_{3/2}^{\text{freeze-in}} h^2 \simeq 10^{-2} \sum_{i: \text{thermalized}} d_i \left( \frac{\tilde{m}_i}{1000 \text{ TeV}} \right)^3 \left( \frac{100 \text{ TeV}}{m_{3/2}} \right), \quad (21)$$

where  $d_i$  is the degrees of freedom of superparticle  $i$  of mass  $\tilde{m}_i \sim \tilde{m}$ . This large freeze-in contribution of Eq. (21) is a characteristic feature of Spread Supersymmetry—values of the cutoff scale  $M_*$  smaller than  $M_{\text{Pl}}$  enhances the couplings between the scalar particles and the Goldstino components of the gravitino, strongly enhancing gravitino production.

The total primordial gravitino abundance is given by the sum of the above two contributions:

$$\Omega_{3/2} = \Omega_{3/2}^{\text{UV}} + \Omega_{3/2}^{\text{freeze-in}}, \quad (22)$$

which determines  $\Omega_{\tilde{W}}^{\text{non-thermal}}$  through Eq. (19). The relic wino LSP abundance is then given by adding the thermal relic contribution, in Eq. (18).

## 3.2 Detecting wino dark matter

### Cosmic ray signals

We now discuss the observability of relic wino LSPs. Since the wino annihilation cross section is relatively large, it can potentially be probed by many processes, such as effects on BBN, distortion of cosmic microwave background (CMB), and production of cosmic rays, even if the wino may not comprise all of the dark matter. In particular, cosmic-ray photon observation by the Fermi collaboration provides a significant constraint on relic winos.

To discuss constraints from indirect detection experiments, including the Fermi observation, it is convenient to define the effective cross section

$$\langle \sigma v \rangle_{\text{eff}} = \left( \frac{\Omega_{\tilde{W}}}{\Omega_{\text{DM}}} \right)^2 \langle \sigma v \rangle_{\tilde{W}}, \quad (23)$$

where  $\langle \sigma v \rangle_{\tilde{W}}$  is the wino annihilation cross section (times velocity). This is the quantity to be compared with the dark matter annihilation cross section in the usual indirect-detection exclusion plots (which assume  $\Omega_{\tilde{W}} = \Omega_{\text{DM}}$ ). The strongest current constraint comes from the Fermi gamma ray search of Milky way satellites [44]. In Fig. 5, we plot the upper bound on  $\Omega_{\tilde{W}}/\Omega_{\text{DM}}$  coming from this constraint as a function of the wino mass. For comparison we show the relic abundance from thermal freeze-out.

Let us discuss the prospect from the future AMS-02 antiproton search, which may provide a very powerful probe for wino dark matter. Wino dark matter annihilations induce high energy antiprotons. However, the flux of antiprotons on the top of the atmosphere strongly depends on the assumptions on the dark matter halo profile and propagation model for the antiproton cosmic rays. Especially, uncertainties from the propagation models are huge and become a factor of

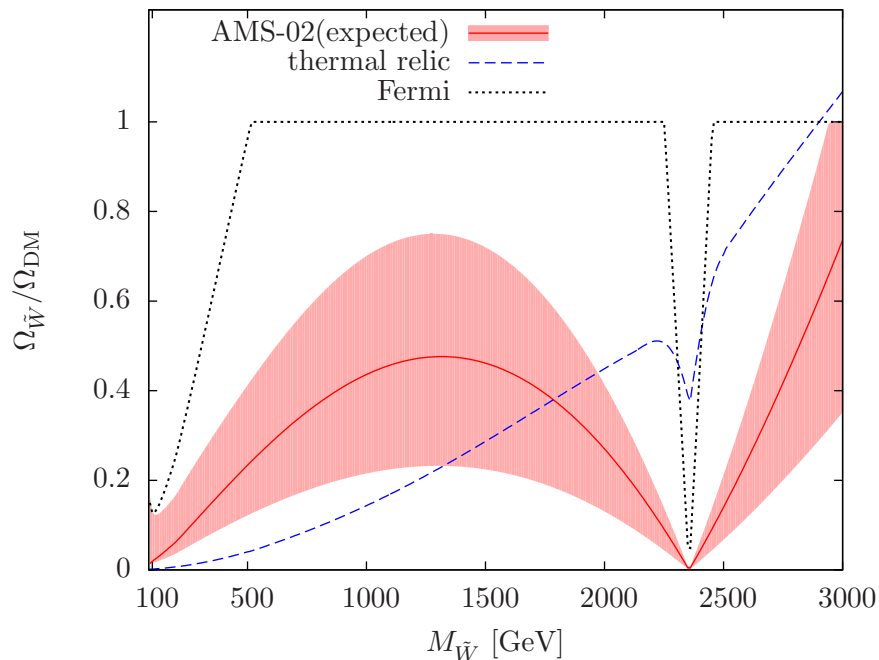


Figure 5: Current and projected upper bounds on  $\Omega_{\tilde{W}}/\Omega_{\text{DM}}$  as a function of the wino mass,  $M_{\tilde{W}}$ , from the Fermi and AMS-02 cosmic ray experiments. The red shaded region shows the current uncertainty coming from the propagation and dark matter halo models. After the AMS-02 experiment, the uncertainty from the cosmic ray propagation will be reduced.

100 [45]. Actually, depending on the propagation parameters, the current antiproton measurement by the PAMELA Collaboration [46] can give a constraint stronger than that of Fermi. The AMS-02 experiment has great advantages not only for measurements of antiprotons but also for other secondary-to-primary ratios such as boron-to-carbon (B/C). High precision measurements of such quantities allow the propagation parameters to be estimated with higher accuracy, drastically reducing the astrophysical uncertainties of the antiproton flux [47]. Hence, AMS-02 will be one of the strongest probes of Spread Supersymmetry.

To estimate the sensitivity of the AMS-02 antiproton search, we have used the programs DRAGON [48] and DarkSUSY [49], to calculate the antiproton fluxes from astrophysical backgrounds and dark matter annihilations. We adopt the value of the acceptance and systematic errors of Ref. [50]. Here we assume the systematic errors come from residual backgrounds, whose rate is 1–10 % of the antiproton signals. For the astrophysical background flux, we use the propagation model KRA of Ref. [45], and we simply assume that uncertainties of the background can be controlled with  $\delta z_t = 1$  kpc, where  $z_t$  is the vertical size of the diffusion zone. This size of the uncertainty will be reasonable after precise measurement of AMS-02 [47]. Since the propagation parameters and the dark matter halo model are not determined well so far, we study some combinations of propagation models (KRA as well as MIN, MED and MAX models in Ref. [51]) and dark matter profiles (NFW and isothermal). We set the local dark matter energy density

$\rho_{\odot} = 0.4 \text{ GeV} \cdot \text{cm}^{-3}$ . Under the above simplified assumptions, we estimate the signal strength to detect deviation from the background at 95 % C.L.. In Fig. 5, we show the sensitivity from the AMS-02 experiment. The solid red line represents the case of KRA+isothermal and the shaded region shows the variation from propagation and dark matter halo models. Note that this uncertainty mainly comes from ignorance of the underlying propagation model, which may be reduced after the experiment.

The current and projected bounds are clearly important especially when the non-thermal contribution in Eq. (17) dominates for low mass wino. For heavier winos ( $\gtrsim 2 \text{ TeV}$ ), AMS-02 may have the potential to probe wino dark matter, even if the relic abundance is purely thermal. This is because resonant process enhances the wino annihilation cross section [24] and heavier winos emit more high energy antiprotons, yielding a signal that is easier to discriminate from the astrophysical background. Note that the results here are obtained under simplified assumptions; in reality, we would need to consider more detailed factors, such as breakdown of power-law primary proton injection, and perform more serious estimates of experimental systematic errors. Nevertheless, these results show that AMS-02 is likely to provide a very powerful probe of Spread Supersymmetry.

## Direct detection

Direct detection of wino dark matter is challenging. The tree-level spin-independent dark matter-nucleon cross section is approximately given by

$$\sigma_{\text{SI}} \simeq (0.6 - 2) \times 10^{-46} \text{ cm}^2 \sin^2(2\beta) \left( \frac{|\mu|}{5 \text{ TeV}} \right)^{-2} \left( \cos(\arg(M_2\mu)) + \left| \frac{M_2}{\mu} \right| \right)^2. \quad (24)$$

In the case that the  $CP$ -violating phase is nearly maximal in the relevant vertex,  $\arg(M_2\mu) \simeq \pi/2$ ,  $\sigma_{\text{SI}}$  is highly suppressed and may be dominated by the second term or loop-induced contributions. For  $\mu \sim 10 \text{ TeV}$ , tree-level and loop-induced contributions are comparable and detailed calculation is required for a precise determination of the cross section. When  $|\mu| \gg 10 \text{ TeV}$ , the cross section is dominated by the loop contribution and  $\sigma_{\text{SI}} \simeq 10^{-47} \text{ cm}^2$ .

The current constraint by the XENON100 experiment is [52]

$$\sigma_{\text{SI}} \lesssim 1 \times 10^{-44} \text{ cm}^2 \left( \frac{M_{\tilde{W}}}{500 \text{ GeV}} \right) \left( \frac{\Omega_{\text{DM}}}{\Omega_{\tilde{W}}} \right), \quad (25)$$

which does not reach the relevant parameter region even for  $\Omega_{\tilde{W}} = \Omega_{\text{DM}}$ .

On the other hand, the projected sensitivity of XENON1T is [53]

$$\sigma_{\text{SI}} \simeq 1 \times 10^{-46} \text{ cm}^2 \left( \frac{M_{\tilde{W}}}{500 \text{ GeV}} \right) \left( \frac{\Omega_{\text{DM}}}{\Omega_{\tilde{W}}} \right), \quad (26)$$

which is comparable with the cross section in Eq. (24) for  $\Omega_{\tilde{W}} = \Omega_{\text{DM}}$ . As can be seen in Fig. 3, for  $r_* > 10$  a wino LSP requires  $|\mu| < m_{3/2}$ . Therefore, future direct dark matter search experiments might detect the wino LSP in the optimistic case that it is the dominant component of dark matter.



## 4 Results and Implications

We now investigate the parameter space of Spread Supersymmetry with wino LSP, based on the discussions so far. We summarize the current status of the model and discuss future prospects for discovery.

### 4.1 The current status

The phenomenology of the model significantly depends on the scale of scalars  $\tilde{m}$ , the gravitino mass  $m_{3/2}$ , the size and phase of the  $\mu$  parameter  $|\mu| = O(m_{3/2})$  and  $\arg(\mu)$ , and  $\tan\beta$ . The first two parameters can be traded with two real numbers  $\sqrt{F_X}$  and  $M_*$ , and the next two with a complex parameter  $L$  in Eq. (10); the value of  $\tan\beta$  can be determined by fixing  $m_h = 125$  GeV. We therefore discuss parameter space of the model in terms of

$$\sqrt{F_X} (= \sqrt{3} m_{3/2} M_{\text{Pl}}), \quad M_* (= \sqrt{3} r_*^{-1} M_{\text{Pl}}), \quad L = \text{Re}L + i \text{Im}L. \quad (27)$$

In particular, the value of  $L$  affects the ratios of the gaugino masses and has significant impacts on implications of the model. The cosmology also depends on the reheating temperature  $T_R$ , so we have 5 parameters in total.

In Figs. 6 – 8, we plot selected physical quantities related to the dark matter and gluino properties in the  $M_*$ - $\sqrt{F_X}$  (or equivalently  $r_*$ - $m_{3/2}$ ) plane for several values for  $T_R$ , assuming that the scalar masses are degenerate with mass  $\tilde{m}$ . (The effect of non-universality will be discussed later.) Specifically, we plot the contours of the gluino decay length  $c\tau_{\tilde{g}}$ , the constraint from Fermi gamma ray search, and the wino relic abundance  $\Omega_{\tilde{W}} h^2$ ; we also plot the contours of the gluino and wino masses  $M_{\tilde{g}, \tilde{W}}$  and the degenerate scalar mass  $\tilde{m}$  in the top left panel of each figure. Here, we have included in the Fermi constraint not only from Milky way satellite search but also from diffuse gamma ray search [54]. Since the cosmic-ray constraint potentially suffers from large astrophysical uncertainties, we also show the three times weaker constraint to be conservative. We also show the future prospect for the AMS-02 antiproton search, using the isothermal dark matter profile. Here we adopt KRA and MIN propagation, which provide medium and more conservative prospect, respectively. We have adopted a renormalization group-improved method for calculation of the gluino decay width [33], and used `micrOMEGAS 2.4` [55] in some parameter regions.

To see general features in the Spread Supersymmetry parameter space, in Figs. 6 and 7 we have chosen two representative values of  $L$ :  $L \simeq 3m_{3/2}$ , which “maximizes” the wino mass keeping the wino LSP, i.e.  $M_{\tilde{W}}$  is only slightly smaller than  $M_{\tilde{B}}$  (Fig. 6) and  $L = 0$ , which corresponds to the case of a pure anomaly-mediated gaugino spectrum (Fig. 7). In a sense, these two cases represent two opposite ends of phenomenology that can be realized in the present model, corresponding to the cases with a small  $M_{\tilde{g}}/M_{\tilde{W}}$  ratio (Fig. 6) and large  $M_{\tilde{g}}/M_{\tilde{W}}$  ratio (Fig. 7). (A true extreme case, however, can occur when  $L \simeq -m_{3/2}$ , in which a cancellation of the anomaly mediated and loop contributions in the wino mass can make  $M_{\tilde{g}}/M_{\tilde{W}}$  really large).

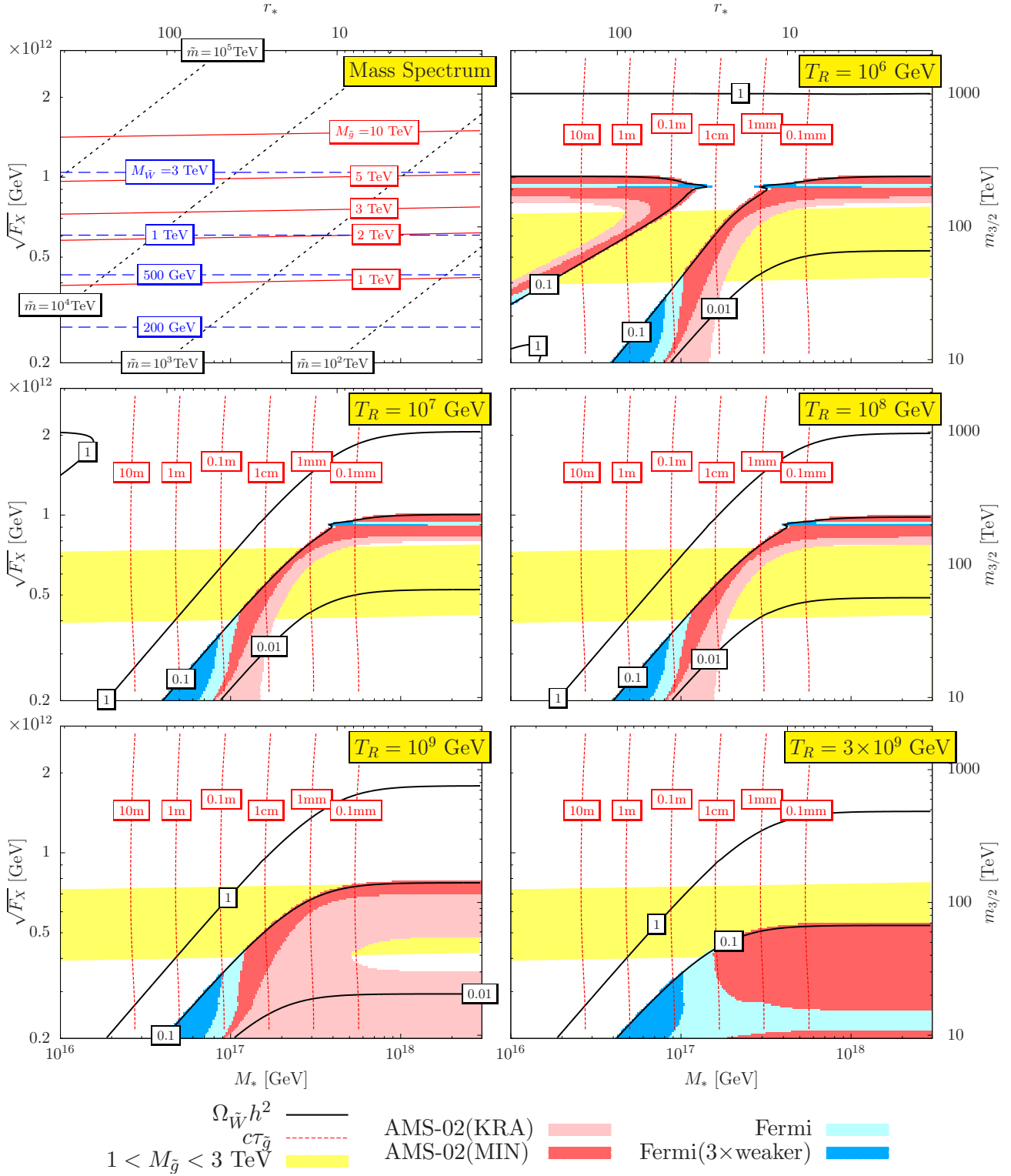


Figure 6: Contours of the gluino decay length  $c\tau_{\tilde{g}}$  and the wino relic abundance  $\Omega_{\tilde{W}} h^2$ , as well as the constraint from the Fermi photon observation and future prospect for the AMS-02 antiproton search, are shown in the  $M_*$ - $\sqrt{F_X}$  (or  $r_*$ - $m_{3/2}$ ) plane for various values of the reheating temperature  $T_R$ . Contours of the gluino- and wino masses  $M_{\tilde{g},\tilde{W}}$  and the degenerate squark mass  $\tilde{m}$  are also shown in the top left panel. The value of  $L$  has been chosen such that  $M_{\tilde{W}}$  is maximized, keeping the wino LSP; numerically,  $L \simeq 3m_{3/2}$ .

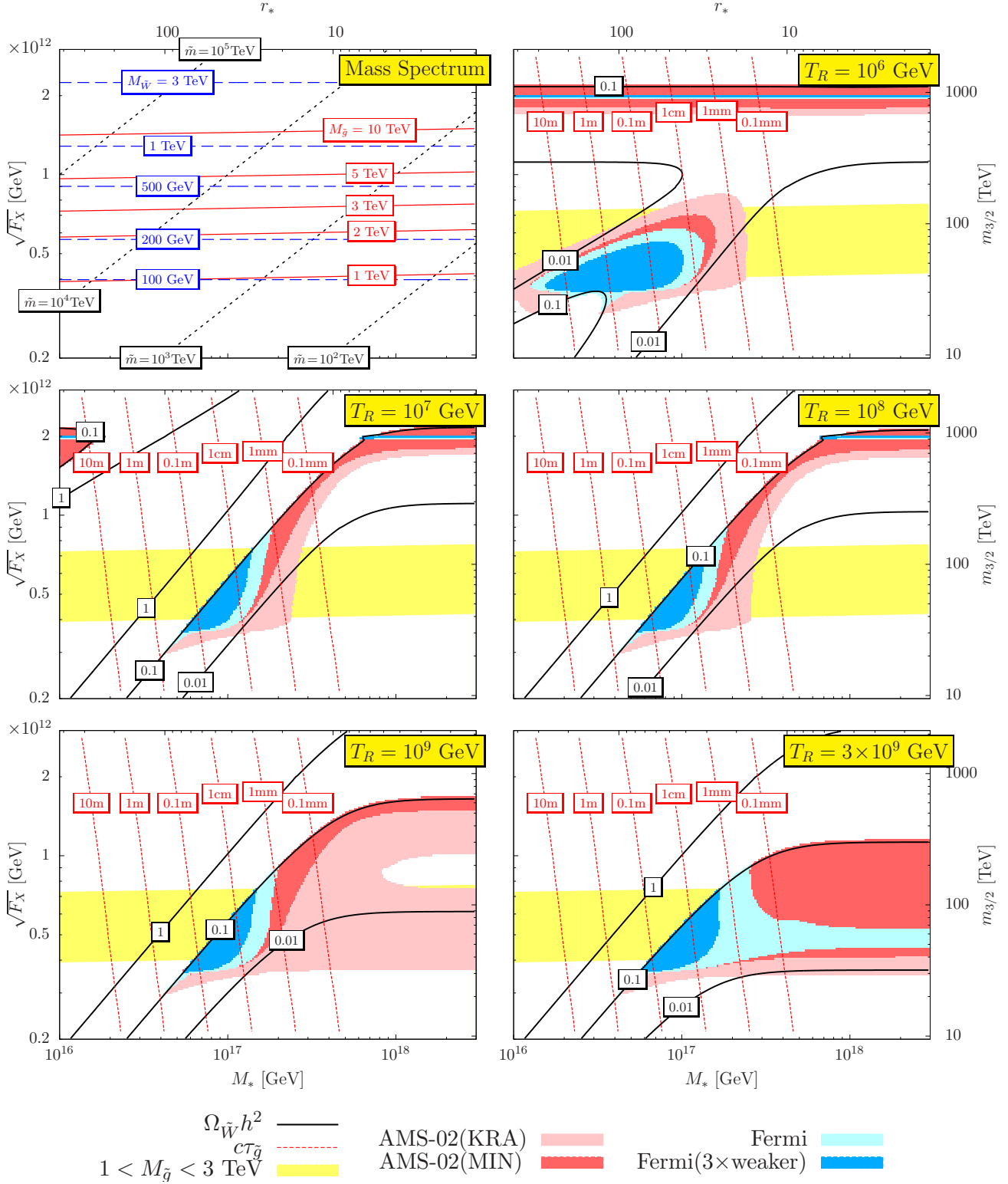


Figure 7: Same as Fig. 6 except that  $L = 0$  (which leads to the purely anomaly mediated gaugino spectrum).

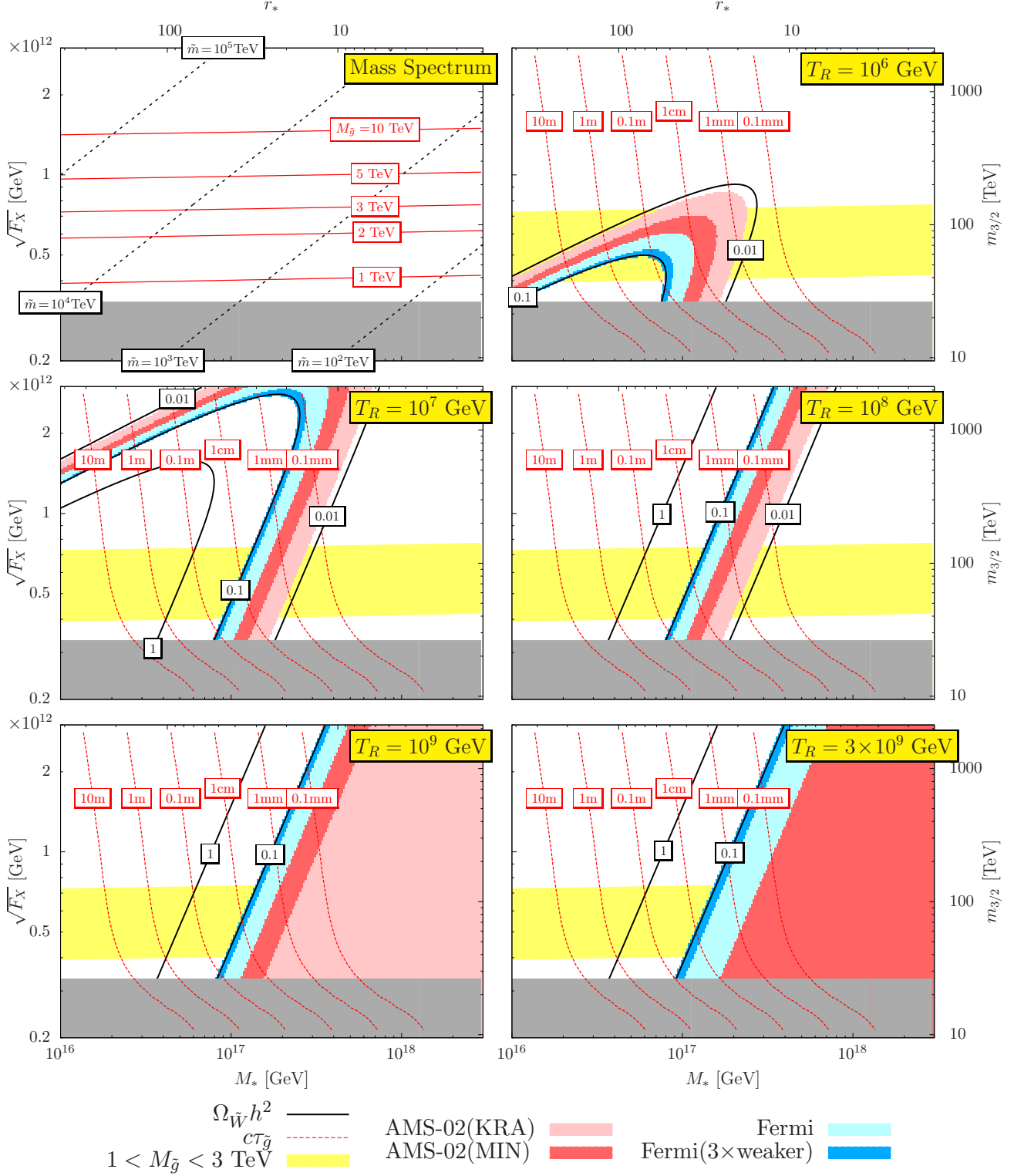


Figure 8: The wino LSP abundance and some physical parameters are shown. We choose  $L$  so that  $M_2 = +300$  GeV. The gray region is the bino LSP.

In both figures, we can see the following general trends. If  $T_R$  is sufficiently lower than  $\tilde{m}$ , e.g. as in the upper-left corner of  $T_R = 10^6$  GeV panels, then the relic wino abundance is controlled only by the thermal freeze-out abundance; hence the contours of constant  $\Omega_{\tilde{W}} h^2$  are horizontal. Once  $T_R$  becomes comparable or larger than  $\tilde{m}$ , however, the freeze-in contribution in Eq. (21) can become important.<sup>6</sup> In particular, this is more effective at larger  $\tilde{m}$ , i.e. smaller  $M_*$  (= larger  $r_*$ ), bending the constant  $\Omega_{\tilde{W}} h^2$  contours downward toward the left (as can be seen clearly in the plots with  $T_R \geq 10^7$  GeV). This effect, therefore, prefers lower superparticle masses for small  $M_*/M_{\text{Pl}} \lesssim O(0.1)$ . For larger  $M_*$ , the contours of constant  $\Omega_{\tilde{W}} h^2$  are horizontal (i.e. do not depend on the scalar masses), which, however, become lower for large  $T_R$  because of the contribution from the decay of the gravitino produced at the reheating, Eq. (20).

The condition from the relic wino abundance, therefore, provides upper bounds on the superparticle masses as a function of  $M_*$  and  $T_R$  for a given  $L$ . For example, in the case of Fig. 6 ( $L \simeq 3m_{3/2}$ ), the gluino mass is bounded very roughly as

$$M_{\tilde{g}} \lesssim \begin{cases} 1 \text{ TeV} \left( \frac{M_*}{10^{17} \text{ GeV}} \right)^{3/2} \left( \frac{\Omega_{\tilde{W}}}{\Omega_{\text{DM}}} \right)^{1/2} & \text{for } M_* \lesssim 10^{17} \text{ GeV}, \\ \min \left\{ 5 \text{ TeV} \left( \frac{\Omega_{\tilde{W}}}{\Omega_{\text{DM}}} \right)^{1/2}, 2 \text{ TeV} \left( \frac{T_R}{3 \times 10^9 \text{ GeV}} \right)^{-1} \left( \frac{\Omega_{\tilde{W}}}{\Omega_{\text{DM}}} \right) \right\} & \text{for } M_* \gtrsim 10^{17} \text{ GeV}. \end{cases} \quad (28)$$

This bound is much tighter than the naive anomaly mediated case of Fig. 7 ( $L = 0$ ):

$$M_{\tilde{g}} \lesssim \begin{cases} 2 \text{ TeV} \left( \frac{M_*}{10^{17} \text{ GeV}} \right)^{3/2} \left( \frac{\Omega_{\tilde{W}}}{\Omega_{\text{DM}}} \right)^{1/2} & \text{for } M_* \lesssim 10^{17} \text{ GeV}, \\ \min \left\{ 20 \text{ TeV} \left( \frac{\Omega_{\tilde{W}}}{\Omega_{\text{DM}}} \right)^{1/2}, 7 \text{ TeV} \left( \frac{T_R}{3 \times 10^9 \text{ GeV}} \right)^{-1} \left( \frac{\Omega_{\tilde{W}}}{\Omega_{\text{DM}}} \right) \right\} & \text{for } M_* \gtrsim 10^{17} \text{ GeV}. \end{cases} \quad (29)$$

We expect that a generic situation of the model is somewhere between these two cases, although larger values of the gluino mass are possible if  $L$  is in the range  $m_{3/2} \lesssim |L| \lesssim 3m_{3/2}$  with  $\arg(L) \simeq \pi$ .

Given that flavor and  $CP$  constraints require rather large  $\tilde{m} > O(10^3 \text{ TeV})$  for generic scalar masses, we may naturally expect a somewhat small cutoff scale,  $M_* \lesssim$  a few  $\times 10^{17}$  GeV. Furthermore, if we require successful thermal leptogenesis, the reheating temperature must be high,  $T_R \gtrsim 2 \times 10^9$  GeV [56]. These select the model to be in particular parameter regions. While the regions start being constrained by the Fermi data, there are still significant regions remaining. The gluino mass in these regions are less than a few TeV for generic values of  $L$ , so we may expect it to be within reach at the 13 TeV run of the LHC. Moreover, the decay length of the gluino in these regions is

$$O(0.1 \text{ mm}) < c\tau_{\tilde{g}} < O(10 \text{ cm}), \quad (30)$$

---

<sup>6</sup>In the calculation of the gravitino abundance in the figures, we have adopted  $\rho_{\text{inf}} \gg \rho_{\text{rad}}$  as the initial condition, where  $\rho_{\text{inf}}$  and  $\rho_{\text{rad}}$  are the inflaton and radiation energy densities. The reason why the freeze-in contribution is relevant even for  $T_R$  slightly smaller than  $\tilde{m}$ , then, is that there are nonzero contributions from scalars heavier than  $T_R$ , which is Boltzmann suppressed after the reheating, and that there is a residuum from the era before the reheating, when  $T \gg T_R$ .

leading to the spectacular signal of a long-lived gluino decaying into a long-lived charged wino having  $c\tau_{\tilde{W}^\pm} = O(10 \text{ cm})$ .

In Fig. 8, we plot the contours of  $c\tau_{\tilde{g}}$  and  $\Omega_{\tilde{W}} h^2$ , together with the Fermi constraint, fixing the wino mass rather than  $L$ :  $M_2 = +300 \text{ GeV}$  (i.e.  $|M_2| = 300 \text{ GeV}$  with  $\arg(M_2) = 0$ ). We also plot the gluino mass  $M_{\tilde{g}}$  and the scalar mass  $\tilde{m}$  in the top left panel. We see that for smaller  $M_*$ , the gluino mass tends to be lighter and its decay length tends to be longer.

So far, we have assumed that the scalar masses are universal, but we generally expect this is not the case. In order to include the effect of non-degeneracy of the scalar masses, we can consider that  $\tilde{m}$  actually represents the “effective scalar mass” appearing in Eq. (21)

$$\tilde{m}_{\text{eff}} = \left( \frac{\sum_i d_i \tilde{m}_i^3}{\sum_i d_i} \right)^{1/3}, \quad (31)$$

and that  $M_*$  and  $r_*$  in these figures are defined by this quantity:

$$M_* \equiv \frac{F_X}{\tilde{m}_{\text{eff}}}, \quad r_* \equiv \frac{\sqrt{3} M_{\text{Pl}} \tilde{m}_{\text{eff}}}{F_X}. \quad (32)$$

The contours of the gluino decay length then represent not those of the true gluino decay length,  $c\tau_{\tilde{g}}$ , but of the “rescaled” gluino decay length

$$c\tau_{\tilde{g},\text{res}} = \tilde{m}_{\text{eff}}^4 \left( \frac{1}{n_{\tilde{q}}} \sum_{\tilde{q}} \frac{1}{m_{\tilde{q}}^4} \right) c\tau_{\tilde{g}}. \quad (33)$$

If there is a significant distribution in the squark masses, the true gluino decay length is then shorter than the values depicted in Figs. 6 – 8, which are obtained assuming universal scalar/squark masses. A hierarchy in the squark spectrum could decouple the gluino lifetime from the cosmological wino abundance, with gluino decay dominated by the lightest squarks and gravitino freeze-in dominated by the heavier ones.

## 4.2 Future prospects

The present model can provide many phenomenological consequences, such as collider signals, dark matter signals, effects on precision physics, and so on. Distinctive features of the model include scalar particles heavier than  $m_{3/2}$  and Higgsinos with mass of order of  $m_{3/2}$  or less. The heavy scalars provide the long-lived gluino, and the relatively lighter Higgsinos provide an enhanced possibility of indirectly detecting the Higgsino sector, compared to the conventional anomaly mediation model. In addition, the wino LSP may not comprise the whole dark matter, implying new possibilities for dark matter detection. Here we discuss future prospects for these signatures.

The LHC has a great reach for the gluino. The production cross section of gluinos is roughly 400, 1 and 0.01 fb for 1, 2 and 3 TeV gluino, respectively. The signature there depends on the gluino lifetime. For  $c\tau_{\tilde{g}} \ll O(1 \text{ mm})$ , the usual search for (missing energy + high  $P_T$  jets) is effective. For

$\sqrt{s} = 14$  TeV and very heavy squarks, the LHC has a discovery reach of  $m_{\tilde{g}}$  up to about 2.0 TeV (2.3 TeV) with an integrated luminosity of  $300 \text{ fb}^{-1}$  ( $3000 \text{ fb}^{-1}$ ) [57, 58]. When  $c\tau_{\tilde{g}} \gtrsim O(0.1 \text{ mm})$ , the displaced vertex from the gluino decay can be recognized. Although the current ATLAS study [59] of the displaced tracks assumes a specific decay topology of  $R$ -parity violation with a muon, a similar detection technique should work here as well for  $c\tau_{\tilde{g}} \gtrsim O(0.1 \text{ mm})$ , since the present model provides similar signals via gluino decay, e.g.  $\tilde{g} \rightarrow \tilde{B}qq \rightarrow \tilde{W}Wqq$ . Applications to different decay topologies, such as displaced vertex + electron, are also expected to work. Note that the gluino lifetime is very sensitive to the squark mass. Therefore, the discovery of gluinos with displaced vertices would have a significant impact on the cosmology of the model, since the squark mass plays a crucial role in determining the dark matter abundance.

Disappearing tracks of charged winos are also interesting signals. As discussed before, in the present model, the decay length of the charged wino may differ from the prediction of the conventional anomaly mediation, because of the contribution from the Higgsino to the charged-neutral wino mass splitting. If the LHC or a future linear collider can determine the precise decay length of the charged wino and/or mass splitting between the charged and neutral winos, it would be possible to explore the Higgsino sector through these measurements.

Other important probes of the model come from the smallness of the  $\mu$  term, which enhances dark matter direct detection as well as EDM detection. The sensitivities of experiments exploring these signals are expected to be drastically improved in the future, enough to probe the case with  $|\mu| \lesssim 10$  TeV as discussed before.

Even if the wino mass is less than about 1 TeV, non-thermal wino production can give a significant relic density, although not necessarily  $\Omega_{\tilde{W}} = \Omega_{\text{DM}}$ , allowing the wino LSP to be probed via cosmic rays and the CMB. In particular, searches for antiproton cosmic rays in AMS-02 is very powerful for detecting signals from wino annihilation. Also, the observation of CMB via the Planck satellite gives significant information of the wino dark matter. In particular, the large cross section of the wino has a great impact on the process of recombination in the early universe, and this effect can be probed via detailed observation of the CMB. The current and expected limits are given by [60, 61]

$$m_{\tilde{W}} \lesssim \left( \frac{\Omega_{\tilde{W}}}{\Omega_{\text{DM}}} \right)^{2/3} \times \begin{cases} 230 \text{ GeV} & (\text{WMAP7}) \\ 460 \text{ GeV} & (\text{Planck forecast}) \\ 700 \text{ GeV} & (\text{cosmic variance with } \ell_{\text{max}} = 2500) \end{cases} \quad (34)$$

at 95 % C.L.. Both experiments are ongoing and will release the data in the near future. Observing  $\Omega_{\tilde{W}} < \Omega_{\text{DM}}$  in these experiments would provide substantial evidence of our model.

Finally, let us discuss another way to test the heavy scalar sector by observations of primordial background gravitational waves. The scalar particles affect the expansion of the universe. At temperatures near  $\tilde{m}$ , a sudden change of relativistic degrees of freedom  $\Delta g_* \sim 100$  is expected, affecting the propagation of background gravitational waves. The next generation of gravitational wave experiments, such as the Deci-hertz Interferometer Gravitational Wave Obser-

vatory (DECIGO) [62] and Big Bang Observer (BBO) [63], have a potential to test this effect if  $\tilde{m} > O(1000 \text{ TeV})$  and the primordial gravitational wave has a large amplitude [64].

## 5 Multiverse Interpretation

While the theoretical structure of Spread Supersymmetry with  $\tilde{W}$  LSP is extremely simple, there is a remarkable coincidence in the value that the key parameters must take for it to be realistic. There are two key mass scales in the theory beyond those of the SM: the supersymmetry breaking scale  $F_X$  that sets  $m_{3/2}$ , and the mediation scale  $M_*$  that then determines  $\tilde{m}$ . In principle these parameters could take values varying over many orders of magnitude. In practice, we see from Figs. 6 and 7 that the region of interest is quite small; if  $\sqrt{F_X} \lesssim 2 \times 10^{11} \text{ GeV}$  the wino would have been discovered at LEP and if  $\sqrt{F_X} \gtrsim 2 \times 10^{12} \text{ GeV}$  there would be too much dark matter. Similarly,  $M_*$  must be within two orders of magnitude of the reduced Planck mass. A third mass scale,  $T_R$ , is crucial for the cosmological abundance of dark matter. This scale is varied over several orders of magnitude in the various panels of Figs. 6 and 7, and is apparently bounded only by  $T_R \lesssim 10^{10} \text{ GeV}$  to avoid too much dark matter from UV production of gravitinos. However, to obtain a baryon asymmetry via thermal leptogenesis requires  $T_R \gtrsim 2 \times 10^9 \text{ GeV}$ , so this mass scale may be tightly constrained also.

The remarkable coincidence is that this small parameter region is precisely where the three independent relic wino production mechanisms (thermal LSP freeze-out, gravitino freeze-in, and UV gravitino production) yield comparable contributions to the dark matter abundance

$$(Ym)_{\tilde{W}}|_{\text{FO}} \sim 10^{-10} \text{ GeV} \left( \frac{\sqrt{F_X}}{2 \times 10^{12} \text{ GeV}} \right)^4 \left( \frac{2 \times 10^{18} \text{ GeV}}{M_{\text{Pl}}} \right)^3, \quad (35)$$

$$(Ym)_{\tilde{W}}|_{\text{FI}} \sim 10^{-10} \text{ GeV} \left( \frac{\sqrt{F_X}}{2 \times 10^{12} \text{ GeV}} \right)^4 \left( \frac{3 \times 10^{17} \text{ GeV}}{M_*} \right)^3, \quad (36)$$

$$(Ym)_{\tilde{W}}|_{\text{UV}} \sim 10^{-10} \text{ GeV} \left( \frac{T_R}{10^9 \text{ GeV}} \right) \left( \frac{\sqrt{F_X}}{2 \times 10^{12} \text{ GeV}} \right)^2 \left( \frac{2 \times 10^{18} \text{ GeV}}{M_{\text{Pl}}} \right)^2. \quad (37)$$

With squark masses of order  $10^3 \text{ TeV}$  the fine-tuning in electroweak symmetry breaking is of order 1 in  $10^8$ , suggesting that the weak scale is anthropically selected. In a multiverse view, the small values of the cosmological constant and the weak scale can both be understood as a consequence of environmental selection; significantly larger values would have catastrophic consequences for large scale structure [8] and for stable nuclei [10]. Could the coincidence of three comparable contributions to LSP dark matter follow from the environmental selection of the relevant mass scales?

Recall that in any version of split supersymmetry the abundance of dark matter has been logically disconnected from the weak scale—there is no “WIMP miracle.” Instead we assume an anthropic requirement on the total energy density of dark matter, either  $\rho > \rho_{\text{cat}}$  or  $\rho < \rho_{\text{cat}}$ , where  $\rho_{\text{cat}}$  is the energy density at some catastrophic boundary, and we consider both possibilities.



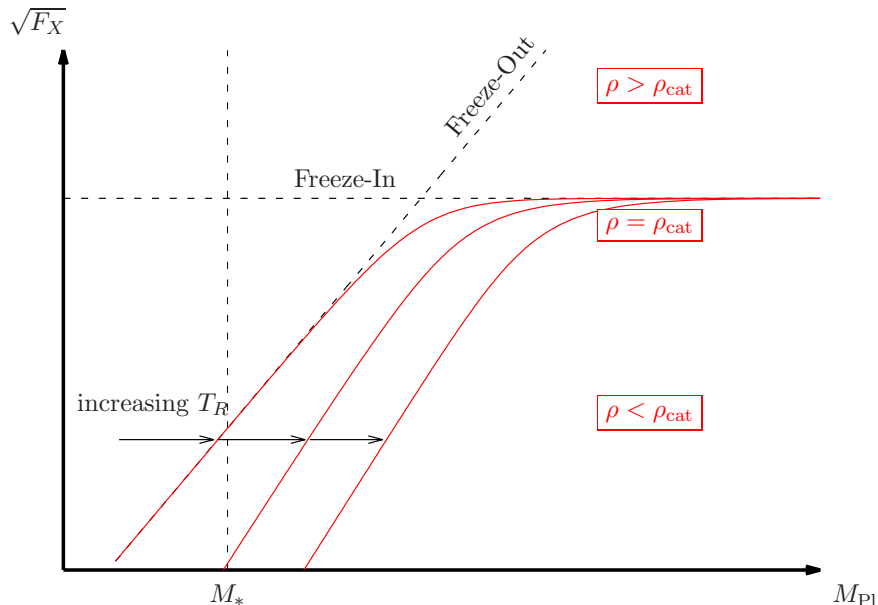


Figure 9: Schematic picture of the catastrophic boundary for the dark matter energy density.

We take  $M_*$  to be the fundamental mass scale of the theory, and consider scanning of  $M_{\text{Pl}}$ ,  $\sqrt{F_X}$  and  $T_R$  over a wide range of values in the multiverse. The red curves in Fig. 9 show the catastrophic boundary  $\rho = \rho_{\text{cat}}$  in the  $(M_{\text{Pl}}, \sqrt{F_X})$  plane for three values of  $T_R$ , assuming that  $\rho_{\text{cat}}$  is a constant, independent of these scanning parameters. For simplicity we begin by fixing  $T_R$  small enough that UV production of gravitinos is negligible, and add scanning of  $T_R$  later, so for now we focus on the upper red curve of Fig. 9. For low values of  $M_{\text{Pl}}$  the boundary is determined by LSP freeze-out, while at higher values it is determined by gravitino freeze-in, which is independent of  $M_{\text{Pl}}$ . Suppose that the environmental requirement is  $\rho < \rho_{\text{cat}}$  and that the multiverse distributions favor a large  $\sqrt{F_X}$  and small  $M_{\text{Pl}}$  such that the most probable universes satisfying the environmental bound are located just below the kink in the catastrophic boundary. This special location is precisely where  $(Ym)_{\tilde{W}}|_{\text{FO}}$  and  $(Ym)_{\tilde{W}}|_{\text{FI}}$  are comparable. Alternatively, if the environmental requirement is  $\rho > \rho_{\text{cat}}$  then the multiverse distributions must favor small values of both  $\sqrt{F_X}$  and  $M_{\text{Pl}}$  for the most probable observed universes to be close to the catastrophic boundary. However, in this case there appears to be runaway behavior along the boundary. However, such a runaway is halted by  $M_{\text{Pl}}$  reaching  $M_*$ . Comparing Eqs. (35) and (36), we see that this happens only an order of magnitude below the kink in the catastrophic boundary. Hence this case also explains the coincidence of comparable freeze-in and freeze-out contributions to dark matter, but favors the freeze-out contribution slightly dominating.

We now add the scanning of  $T_R$  to the above picture. For  $T_R < 10^8$  GeV,  $(Ym)_{\tilde{W}}|_{\text{UV}}$  is subdominant so that the catastrophic boundary is essentially unaltered and is the upper red curve of Fig. 9. However for larger values of  $T_R$ , the catastrophic boundary at lower values of  $M_{\text{Pl}}$  is pushed

down to lower  $\sqrt{F_X}$  by UV production of gravitinos, as shown by the two lower red curves in Fig. 9. If the environmental requirement is  $\rho > \rho_{\text{cat}}$ , it is not possible to understand the triple coincidence of freeze-out, freeze-in, and UV contributions—if the multiverse distribution favors small  $T_R$  the UV contribution is negligible, while if it prefers high  $T_R$  there is runaway behavior to high  $T_R$  and low  $\sqrt{F_X}$ . However, if the environmental requirement is  $\rho < \rho_{\text{cat}}$ , the triple coincidence is easy to understand. If the multiverse prefers large  $T_R$ , but with a distribution that is not as strong as that for large  $\sqrt{F_X}$  and small  $M_{\text{Pl}}$ , then the most probable value of  $T_R$  will be where it just starts to affect the catastrophic boundary with  $T_R$  near  $10^9$  GeV. If the catastrophic boundary is drawn as a surface in  $(M_{\text{Pl}}, \sqrt{F_X}, T_R)$  space, the triple coincidence occurs in universes that lie near the “tip of the cone” of this surface [65]. With right-handed neutrino masses scanning with a distribution favoring large values, then an anthropic requirement of sufficient baryon asymmetry will force at least one right-handed neutrino mass to be at the  $10^9$  GeV scale.

If the physics of the catastrophic boundary for dark matter depends on gravity, or on the expansion rate of the universe, then we expect  $\rho_{\text{cat}}$  to depend on  $M_{\text{Pl}}$ , changing the location of the boundary in Fig. 9. However, providing the dependence on  $M_{\text{Pl}}$  is rather featureless, for example a simple power law, the boundary will simply appear rotated in Fig. 9, and will still display the crucial kink. If the probability distribution grows towards the kink then the understanding of the coincidences is preserved. For example, for  $\rho < \rho_{\text{cat}} \propto 1/M_{\text{Pl}}^n$ , with  $n = 1, 2$ , the coincidence results providing the strongest distribution favors large  $\sqrt{F_X}$ .

Finally, it has recently been shown that in a theory such as ours, with  $|\mu| < \tilde{m} \ll M_*$ , a somewhat special boundary condition on the top squark and up-type Higgs masses at the scale  $M_*$  is required to avoid color breaking minima while allowing electroweak symmetry breaking [66]. However, if electroweak symmetry breaking and color conservation are viewed as environmental requirements on a multiverse, then this region of scalar masses will be selected environmentally in the multiverse.

## 6 Conclusion

Spread Supersymmetry with wino LSP is a particularly simple theory of Split Supersymmetry resulting from the supersymmetry breaking of Eq. (1), leading to the typical spectrum shown in Fig. 1. The squarks are within about an order of magnitude of  $10^3$  TeV and  $\tan\beta$  is expected to be order unity, leading to a prediction for the mass of a SM-like Higgs boson shown in Fig. 2. The recent discovery of a 125 GeV SM-like Higgs boson strongly motivates further study of this theory.

Our key results are shown in Figs. 6 and 7 for two different values of  $\mu$ : these two figures represent opposite extremes of the expected phenomenology, with Fig. 6 (7) having a small (large) gluino to wino mass ratio. The solid black lines show our results for the cosmological wino abundance, the red dashed lines show our predictions for the gluino lifetime and the yellow bands show regions with the gluino mass in the (1 – 3) TeV, in reach of the LHC. If the fundamental mass

scale,  $M_*$ , that acts as a cutoff to the effective theory and is the mediation scale for supersymmetry breaking, is of order the Planck scale, then gluino decays are always prompt. Also, in this case if  $\Omega_{\tilde{W}}h^2 \simeq 0.1$  the gluinos are too heavy to discover at the LHC, unless  $T_R$  is near its maximal value of order  $10^9$  GeV.

In Spread Supersymmetry, however, allowing for smaller values of  $M_*$  opens up a region of parameter space with interesting experimental signatures. Requiring that the wino abundance  $\Omega_{\tilde{W}}h^2 < 0.1$ , we find  $M_* > 2 \times 10^{16}$  GeV throughout the region, preserving a highly successful gauge coupling unification. The resulting region of interest has some dependence on both  $\mu$  and  $T_R$ . Crucially, a large fraction of this region with  $T_R > \tilde{m}$  has gluinos within reach of LHC. Furthermore, provided the squark spectrum is not too hierarchical, in a large fraction of the region gluinos decay with displaced vertices. Gluino decays also lead to tracks from long-lived charged winos and may give flavor violating signals.

Much of this allowed region has  $\Omega_{\tilde{W}}h^2 > 0.01$ , as expected in theories where dark matter is environmentally selected in the multiverse. AMS-02 searches for cosmic ray antiprotons will provide an important probe of this region.

## Acknowledgments

S.S. thanks N. Nagata for valuable discussions. This work was supported in part by the Director, Office of Science, Office of High Energy and Nuclear Physics, of the US Department of Energy under Contracts DE-FG02-05ER41360 and DE-AC02-05CH11231, in part by the National Science Foundation under grants PHY-0855653 and PHY-1002399 and in part by the EU ITN grant UNILHC 237920 (Unification in the LHC era). L.J.H. and Y.N. acknowledge the hospitality of the Aspen Center for Physics, which is supported by the National Science Foundation Grant No. PHY-1066293.

## References

- [1] A. H. Chamseddine, R. Arnowitt and P. Nath, Phys. Rev. Lett. **49**, 970 (1982); R. Barbieri, S. Ferrara and C. A. Savoy, Phys. Lett. B **119**, 343 (1982); L. Hall, J. Lykken and S. Weinberg, Phys. Rev. D **27**, 2359 (1983).
- [2] P. Hořava and E. Witten, Nucl. Phys. B **460**, 506 (1996) [hep-th/9510209]; Nucl. Phys. B **475**, 94 (1996) [hep-th/9603142]; E. Witten, Nucl. Phys. B **471**, 135 (1996) [hep-th/9602070].
- [3] M. Y. Khlopov and A. D. Linde, Phys. Lett. B **138**, 265 (1984); J. Ellis, J. E. Kim and D. V. Nanopoulos, Phys. Lett. B **145**, 181 (1984).
- [4] M. Kawasaki, K. Kohri, T. Moroi and A. Yotsuyanagi, Phys. Rev. D **78**, 065011 (2008) [arXiv:0804.3745 [hep-ph]].

- [5] L. Randall and R. Sundrum, Nucl. Phys. B **557**, 79 (1999) [arXiv:hep-th/9810155].
- [6] G. F. Giudice, M. A. Luty, H. Murayama and R. Rattazzi, JHEP **12**, 027 (1998) [arXiv:hep-ph/9810442].
- [7] J. D. Wells, hep-ph/0306127; Phys. Rev. D **71**, 015013 (2005) [hep-ph/0411041].
- [8] S. Weinberg, Phys. Rev. Lett. **59**, 2607 (1987); see also, T. Banks, Nucl. Phys. B **249**, 332 (1985); A. D. Linde, Rept. Prog. Phys. **47**, 925 (1984).
- [9] H. Martel, P. R. Shapiro and S. Weinberg, Astrophys. J. **492**, 29 (1998) [arXiv:astro-ph/9701099]; G. Larsen, Y. Nomura and H. L. L. Roberts, Phys. Rev. D **84**, 123512 (2011) [arXiv:1107.3556 [hep-th]].
- [10] V. Agrawal, S. M. Barr, J. F. Donoghue and D. Seckel, Phys. Rev. D **57**, 5480 (1998) [arXiv:hep-ph/9707380].
- [11] R. Bousso and J. Polchinski, JHEP **06**, 006 (2000) [arXiv:hep-th/0004134]; S. Kachru, R. Kallosh, A. Linde and S. P. Trivedi, Phys. Rev. D **68**, 046005 (2003) [arXiv:hep-th/0301240]; L. Susskind, arXiv:hep-th/0302219; M. R. Douglas, JHEP **05**, 046 (2003) [arXiv:hep-th/0303194].
- [12] N. Arkani-Hamed and S. Dimopoulos, JHEP **06**, 073 (2005) [arXiv:hep-th/0405159].
- [13] L. J. Hall and Y. Nomura, JHEP **03**, 076 (2010) [arXiv:0910.2235 [hep-ph]].
- [14] See, e.g., M. Papucci, J. T. Ruderman and A. Weiler, arXiv:1110.6926 [hep-ph]; L. J. Hall, D. Pinner and J. T. Ruderman, JHEP **04**, 131 (2012) [arXiv:1112.2703 [hep-ph]]; for earlier work, see R. Kitano and Y. Nomura, Phys. Rev. D **73**, 095004 (2006) [hep-ph/0602096].
- [15] N. Arkani-Hamed, A. Delgado and G. F. Giudice, Nucl. Phys. B **741**, 108 (2006) [hep-ph/0601041].
- [16] Y. Nomura, JHEP **11**, 063 (2011) [arXiv:1104.2324 [hep-th]]; arXiv:1110.4630 [hep-th]; Astron. Rev. **7**, 36 (2012) [arXiv:1205.2675 [hep-th]].
- [17] L. J. Hall and Y. Nomura, JHEP **01**, 082 (2012) [arXiv:1111.4519 [hep-ph]].
- [18] G. F. Giudice and A. Masiero, Phys. Lett. B **206**, 480 (1988); J. A. Casas and C. Muñoz, Phys. Lett. B **306**, 288 (1993) [arXiv:hep-ph/9302227].
- [19] L. Hall, J. Lykken and S. Weinberg, in Ref. [1]; L. J. Hall, Proc. Winter School (Mahabaleshwar, India), eds. P. Roy and V. Singh, Lecture Notes in Physics, Vol. 208 (Springer, Berlin, 1984) p. 197.
- [20] R. Hempfling, Phys. Lett. B **329**, 222 (1994) [arXiv:hep-ph/9404257]; J. E. Kim and H. P. Nilles, Mod. Phys. Lett. A **9**, 3575 (1994) [arXiv:hep-ph/9406296]; L. J. Hall, Y. Nomura and A. Pierce, Phys. Lett. B **538**, 359 (2002) [arXiv:hep-ph/0204062].
- [21] T. Gherghetta, G. F. Giudice and J. D. Wells, Nucl. Phys. B **559**, 27 (1999) [hep-ph/9904378]; T. Moroi and L. Randall, Nucl. Phys. B **570**, 455 (2000) [hep-ph/9906527].

- [22] J. Hisano, S. Matsumoto, O. Saito and M. Senami, Phys. Rev. D **73**, 055004 (2006) [hep-ph/0511118]; J. Hisano, S. Matsumoto, M. Nagai, O. Saito and M. Senami, Phys. Lett. B **646**, 34 (2007) [hep-ph/0610249].
- [23] J. Hisano, K. Ishiwata and N. Nagata, Phys. Rev. D **82**, 115007 (2010) [arXiv:1007.2601 [hep-ph]]; J. Hisano, K. Ishiwata, N. Nagata and T. Takesako, JHEP **07**, 005 (2011) [arXiv:1104.0228 [hep-ph]]; R. J. Hill and M. P. Solon, Phys. Lett. B **707**, 539 (2012) [arXiv:1111.0016 [hep-ph]].
- [24] J. Hisano, S. Matsumoto, M. M. Nojiri and O. Saito, Phys. Rev. D **71**, 063528 (2005) [hep-ph/0412403].
- [25] M. Ibe, T. Moroi and T. T. Yanagida, Phys. Lett. B **644**, 355 (2007) [hep-ph/0610277]; M. R. Buckley, L. Randall and B. Shuve, JHEP **05**, 097 (2011) [arXiv:0909.4549 [hep-ph]].
- [26] S. Asai, T. Moroi, K. Nishihara and T. T. Yanagida, Phys. Lett. B **653**, 81 (2007) [arXiv:0705.3086 [hep-ph]]; S. Asai, T. Moroi and T. T. Yanagida, Phys. Lett. B **664**, 185 (2008) [arXiv:0802.3725 [hep-ph]]; S. Asai, Y. Azuma, O. Jinnouchi, T. Moroi, S. Shirai and T. T. Yanagida, Phys. Lett. B **672**, 339 (2009) [arXiv:0807.4987 [hep-ph]].
- [27] M. Ibe and T. T. Yanagida, Phys. Lett. B **709**, 374 (2012) [arXiv:1112.2462 [hep-ph]]; M. Ibe, S. Matsumoto and T. T. Yanagida, Phys. Rev. D **85**, 095011 (2012) [arXiv:1202.2253 [hep-ph]]; B. Bhattacharjee, B. Feldstein, M. Ibe, S. Matsumoto and T. T. Yanagida, arXiv:1207.5453 [hep-ph].
- [28] N. Arkani-Hamed, S. Dimopoulos, G. F. Giudice and A. Romanino, Nucl. Phys. B **709**, 3 (2005) [hep-ph/0409232].
- [29] L. J. Hall, K. Jedamzik, J. March-Russell and S. M. West, JHEP **03**, 080 (2010) [arXiv:0911.1120 [hep-ph]]; C. Cheung, G. Elor and L. Hall, Phys. Rev. D **84**, 115021 (2011) [arXiv:1103.4394 [hep-ph]].
- [30] A. D. Linde, Phys. Lett. B **201**, 437 (1988); F. Wilczek, arXiv:hep-ph/0408167; M. Tegmark, A. Aguirre, M. J. Rees and F. Wilczek, Phys. Rev. D **73**, 023505 (2006) [arXiv:astro-ph/0511774].
- [31] See, e.g., G. Dvali, Fortsch. Phys. **58**, 528 (2010) [arXiv:0706.2050 [hep-th]], and references therein.
- [32] M. Toharia and J. D. Wells, JHEP **02**, 015 (2006) [hep-ph/0503175].
- [33] P. Gambino, G. F. Giudice and P. Slavich, Nucl. Phys. B **726**, 35 (2005) [hep-ph/0506214].
- [34] R. Sato, S. Shirai and K. Tobioka, arXiv:1207.3608 [hep-ph].
- [35] ATLAS Collaboration, ATLAS-CONF-2012-109.
- [36] ATLAS Collaboration, ATLAS-CONF-2012-058.

- [37] S. Chatrchyan *et al.* [CMS Collaboration], arXiv:1207.0106 [hep-ex].
- [38] S. Chatrchyan *et al.* [CMS Collaboration], arXiv:1205.0272 [hep-ex].
- [39] See, e.g., F. Gabbiani, E. Gabrielli, A. Masiero and L. Silvestrini, Nucl. Phys. B **477**, 321 (1996) [hep-ph/9604387].
- [40] J. J. Hudson, D. M. Kara, I. J. Smallman, B. E. Sauer, M. R. Tarbutt and E. A. Hinds, Nature **473**, 493 (2011).
- [41] See, e.g., A. C. Vutha *et al.*, J. Phys. B **43**, 074007 (2010) [arXiv:0908.2412 [physics.atom-ph]].
- [42] J. Pradler and F. D. Steffen, Phys. Lett. B **648**, 224 (2007) [hep-ph/0612291].
- [43] V. S. Rychkov and A. Strumia, Phys. Rev. D **75**, 075011 (2007) [hep-ph/0701104].
- [44] M. Ackermann *et al.* [Fermi-LAT Collaboration], Phys. Rev. Lett. **107**, 241302 (2011) [arXiv:1108.3546 [astro-ph.HE]].
- [45] C. Evoli, I. Cholis, D. Grasso, L. Maccione and P. Ullio, Phys. Rev. D **85**, 123511 (2012) [arXiv:1108.0664 [astro-ph.HE]].
- [46] O. Adriani *et al.* [PAMELA Collaboration], Phys. Rev. Lett. **105**, 121101 (2010) [arXiv:1007.0821 [astro-ph.HE]].
- [47] M. Pato, D. Hooper and M. Simet, JCAP **06**, 022 (2010) [arXiv:1002.3341 [astro-ph.HE]].
- [48] C. Evoli, D. Gaggero, D. Grasso and L. Maccione, JCAP **10**, 018 (2008) [arXiv:0807.4730 [astro-ph]].
- [49] P. Gondolo, J. Edsjö, P. Ullio, L. Bergstrom, M. Schelke and E. A. Baltz, JCAP **07**, 008 (2004) [astro-ph/0406204].
- [50] A. G. Malinin [AMS Collaboration], Phys. Atom. Nucl. **67**, 2044 (2004).
- [51] T. Delahaye, R. Lineros, F. Donato, N. Fornengo and P. Salati, Phys. Rev. D **77**, 063527 (2008) [arXiv:0712.2312 [astro-ph]].
- [52] E. Aprile *et al.* [XENON100 Collaboration], arXiv:1207.5988 [astro-ph.CO].
- [53] E. Aprile [XENON1T Collaboration], arXiv:1206.6288 [astro-ph.IM].
- [54] M. Ackermann *et al.* [Fermi-LAT Collaboration], Phys. Rev. D **86**, 022002 (2012) [arXiv:1205.2739 [astro-ph.HE]].
- [55] G. Bélanger *et al.*, Comput. Phys. Commun. **182**, 842 (2011) [arXiv:1004.1092 [hep-ph]]; G. Bélanger, F. Boudjema, A. Pukhov and A. Semenov, Comput. Phys. Commun. **149**, 103 (2002) [hep-ph/0112278]; Comput. Phys. Commun. **174**, 577 (2006) [hep-ph/0405253].
- [56] G. F. Giudice, A. Notari, M. Raidal, A. Riotto and A. Strumia, Nucl. Phys. B **685**, 89 (2004) [hep-ph/0310123].
- [57] H. Baer, V. Barger, A. Lessa and X. Tata, arXiv:1207.4846 [hep-ph].

- [58] ATLAS Collaboration, ATL-PHYS-PUB-2012-001.
- [59] ATLAS Collaboration, ATLAS-CONF-2012-113.
- [60] S. Galli, F. Iocco, G. Bertone and A. Melchiorri, Phys. Rev. D **80**, 023505 (2009) [arXiv:0905.0003 [astro-ph.CO]]; Phys. Rev. D **84**, 027302 (2011) [arXiv:1106.1528 [astro-ph.CO]].
- [61] T. R. Slatyer, N. Padmanabhan and D. P. Finkbeiner, Phys. Rev. D **80**, 043526 (2009) [arXiv:0906.1197 [astro-ph.CO]].
- [62] [http://tamago.mtk.nao.ac.jp/decigo/index\\_E.html](http://tamago.mtk.nao.ac.jp/decigo/index_E.html)
- [63] S. Phinney *et al.*, NASA mission concept study (2004).
- [64] R. Saito and S. Shirai, Phys. Lett. B **713**, 237 (2012) [arXiv:1201.6589 [hep-ph]].
- [65] L. J. Hall and Y. Nomura, Phys. Rev. D **78**, 035001 (2008) [arXiv:0712.2454 [hep-ph]]; R. Bousso, L. J. Hall and Y. Nomura, Phys. Rev. D **80**, 063510 (2009) [arXiv:0902.2263 [hep-th]].
- [66] A. Arvanitaki, N. Craig, S. Dimopoulos and G. Villadoro, arXiv:1210.0555 [hep-ph].